Cite this: DOI: 10.1039/c0xx00000x

www.rsc.org/xxxxxx

View Article Online
DOI: 10.1039/C3GC41666F
PAPER

One-pot combination of enzyme and Pd nanoparticle catalysis for the synthesis of enantiomerically pure 1,2-amino alcohols

Joerg H. Schrittwieser,*[a] Francesca Coccia,[b] Selin Kara,[a] Barbara Grischek,[c] Wolfgang Kroutil,[c] Nicola d'Alessandro[d] and Frank Hollmann*[a]

Received (in XXX, XXX) Xth XXXXXXXXX 20XX, Accepted Xth XXXXXXXXX 20XX
DOI: 10.1039/b000000x

One-pot combinations of sequential catalytic reactions can offer practical and ecological advantages over classical multi-step synthesis schemes. In this context, the integration of enzymatic and chemo-catalytic transformations holds particular potential for efficient and selective reaction sequences that would not be possible using either method alone. Here we report the one-pot combination of alcohol dehydrogenase-catalysed asymmetric reduction of 2-azido ketones and Pd nanoparticle-catalysed hydrogenation of the resulting azido alcohols, which gives access to both enantiomers of aromatic 1,2-amino alcohols in high yields and excellent optical purity (*ee* >99%). Furthermore, we demonstrate the incorporation of an upstream azidolysis and a downstream acylation step into the one-pot system, thus establishing a highly integrated synthesis of the antiviral natural product (*S*)-tembamide in 73% yield (*ee* >99%) over 4 steps. Avoiding the purification and isolation of intermediates in this synthetic sequence leads to an unprecedentedly low ecological footprint, as quantified by E-factor and solvent demand.

Introduction

The integration of several chemical transformations into one-pot processes (often referred to as 'domino', 'tandem', or 'cascade' systems) offers advantages with respect to operational simplicity, operating time and costs, safety, and the consumption of energy and materials.[1] From an ecological perspective, the one-pot combination of catalytic methods[2] is particularly appealing, and recent years have brought about remarkable developments in the use of heterogeneous, homogeneous, organo- and biocatalysts in cascade systems.[3] However, these approaches typically remain within one individual 'subfield' of catalysis, while the one-pot combination of different types of catalysts is less explored. This is particularly true for combinations of chemical catalysts and enzymes, which are often complicated by divergent reaction conditions and detrimental interactions of the bio- and chemo-catalysts.[4] Nevertheless, several excellent recent studies aimed at bringing chemo- and biocatalysis closer together clearly demonstrate the potential of chemo-enzymatic one-pot systems.[5] In this context, true cascades – in which the biocatalytic and chemical reactions proceed concurrently – definitely represent the most elegant examples, but they are also most prone to the above-mentioned difficulties.[6] Sequential chemo-enzymatic one-pot reactions are more easily realised and offer essentially the same environmental advantages (*e.g.* reduction of solvent use due to elimination of work-up and purification steps).[4a,4c,7]

The 2-amino-1-aryl alcohol moiety is a common structural motif in biologically active compounds,[8] as it forms the basic scaffold of adrenergics (*e.g.* the hormones adrenaline and noradrenaline, β-adrenergic blockers, and anti-asthma drugs), amphenicol antibiotics, and several bioactive natural products (Fig. 1). In addition, 1,2-amino alcohols have found broad use as chiral ligands and auxiliaries in asymmetric synthesis.[9] For both pharmaceutical and synthetic applications, a high optical purity of chiral amino alcohols is desired, posing the need for highly selective asymmetric syntheses of these compounds. Chemical methods – such as asymmetric hydrogenation[10] or transfer hydrogenation[11] of 2-amino ketones or their synthetic equivalents – have been intensively studied in recent years, yet they often fail to afford enantiomerically pure products. As a result, classical resolution is still a widely used technique in the preparation of chiral 1,2-amino alcohols, either for upgrading the *ee* of an optically enriched product or for resolving the racemate.[10a]

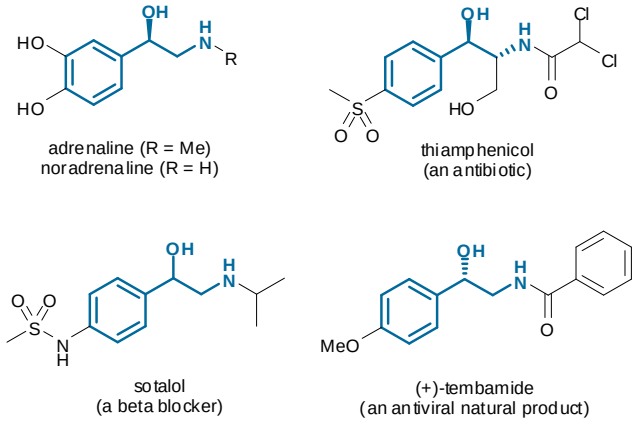

Fig. 1 Examples of biologically active 1,2-amino alcohols (2-amino-1-aryl alcohol motif highlighted in bold)

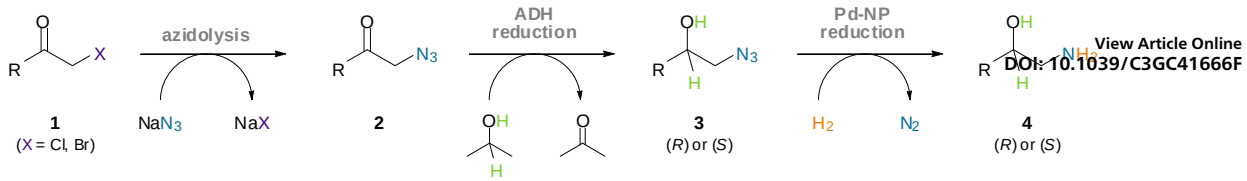

a: R = Ph, X = Cl; **b:** R = 4-Cl-C$_6$H$_4$, X = Br; **c:** R = 4-F-C$_6$H$_4$, X = Br; **d:** R = 4-tolyl, X = Br; **e:** R = 4-MeO-C$_6$H$_4$, X = Br; **f:** R = 2-furyl, X = Br

Scheme 1 Chemo-enzymatic approach towards optically pure 1,2-amino alcohols *via* azidolysis, alcohol dehydrogenase (ADH) catalysed asymmetric reduction, and Pd nanoparticle (Pd-NP) catalysed azide hydrogenation

Biocatalysis, on the other hand, offers several options for the preparation of optically pure 1,2-amino alcohols in general, such as kinetic resolution or dynamic kinetic resolution of the racemate using lipases,[12] oxidative kinetic resolution of *N*-protected amino ketones by Baeyer–Villiger monooxygenases,[13] the combination of aldolase-catalysed C–C bond formation and enzymatic decarboxylation,[14] or the combination of lyase-catalysed C–C bond formation with reductive amination catalysed by ω-transaminases.[15] However, biocatalytic asymmetric methods for the preparation of 2-amino-1-aryl alcohols in particular are comparably scarce.[12e,14,15a,16a]

Herein, we describe a chemo-enzymatic approach for the asymmetric synthesis of this important substance class: a sequential one-pot combination of stereoselective azido ketone reduction by alcohol dehydrogenases and subsequent azide hydrogenation by palladium nanoparticles (Scheme 1), which provides access to both enantiomers of 2-amino-1-aryl alcohols in high yields and with excellent optical purities. The integration of an upstream azido-lysis step into the one-pot process and *in situ* benzoylation of the crude amino alcohol have also been achieved, enabling the one-pot asymmetric synthesis of the natural product tembamide (Fig. 1) in four steps from the corresponding commercially available bromo ketone **1e**. The ecological benefits of this one-pot concept are demonstrated by a basic environmental impact assessment.

Results and Discussion

Azido alcohol hydrogenation catalysed by metal nanoparticles

In our one-pot approach, we envisioned to combine the asymmetric reduction of 2-azido ketones catalysed by alcohol dehydrogenases (ADHs) with azide hydrogenation catalysed by recently reported[17] lignin-stabilised metal nanoparticles (NPs). Since the latter reaction had not been investigated before, we began our studies with screening six different metal nanoparticle preparations (Pd or Pt, stabilised by three different lignin varieties) in the hydrogenation of 2-azido-1-phenylethanol **3a**. Phosphate buffer containing 5% (v/v) of 2-propanol as organic co-solvent was chosen as reaction medium to ensure compatibility with the conditions for the enzyme-catalysed step. As shown in Table 1, Pd-LC and Pd-LK nanoparticles (for explanation of nanoparticle types, see Table 1 footnotes) gave the best results, leading to full conversion within 4 h (Entries 1 and 3). Minor amounts of unidentified side products were formed in all reactions, but subsequent experiments showed that by carrying out the reduction under basic conditions (pH 9) the chemoselectivity can be raised further, such that 2-amino-1-phenylethanol **4a** was the only product detectable by GC–FID and NMR analysis (Table 1, Entry 7). The hydrogenation of **3b–f** under identical conditions proceeded with the same high level of selectivity, affording the corresponding 1,2-amino alcohols **4b–f** in essentially pure form.[18]

Asymmetric azido ketone reduction catalysed by ADHs

Next, we turned our attention to the ADH-catalysed asymmetric reduction of aromatic 2-azido ketones. Although there is literature precedence for this transformation,[19] a broad survey of suitable enzymes has not yet been reported. Therefore, we carried out an extensive screening of 79 commercial ADHs of unspecified origin and four bacterial ADHs (ADH-A from *Rhodococcus ruber* DSM 44541, *Tb*ADH from *Thermoanaerobium brockii*, *Lk*ADH from *Lactobacillus kefir*, *Lb*ADH from *Lactobacillus brevis*)[20] in the reduction of **2a** to **3a**. The screening was performed at 50 mM concentration of **2a** and in the presence of 5% (v/v) 2-propanol, the latter serving both as co-solvent and co-substrate. Table 2 shows selected results of the ADH screening (for complete results, see ESI). As a general trend, we identified more anti-Prelog-selective[21,22] ADHs (18) with activity on **2a** than Prelog-selective ones (9), and on average the former showed about 5–10 times higher activity than the latter. Only ten enzymes afforded optically pure **3a**, whereby four gave the (*R*)-enantiomer and six the (*S*)-enantiomer.[23] Based on the observed activities and stereoselectivities we considered the commercial ADHs listed in Table 2 (Entries 5–8) as well as ADH-A (Entry 1) the most promising biocatalysts for the reaction under study.

Table 1 Hydrogenation of **3a** to **4a** catalysed by different types of lignin-stabilised metal nanoparticles[a]

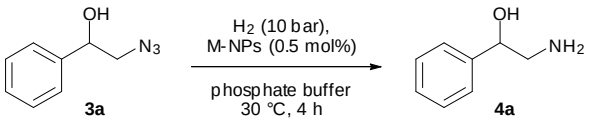

Entry	NP type[b]	Conversion [%][c]	Selectivity [%][c]
1	Pd–LC	>99	86
2	Pd–LA	95	89
3	Pd–LK	>99	85
4	Pt–LC	52	89
5	Pt–LA	97	85
6	Pt–LK	97	87
7	Pd–LK[d]	>99	>99

[a] Conditions: 100 mM **3a**, 0.5 mM NPs, 10 bar H_2, 30 °C, 4 h. For details, see Experimental Section. [b] Lignin varieties: LC = sulfonated lignin with Ca^{2+} counterions, LA = sulfonated lignin with NH^{4+} counterions, LK = low-sulfonate Kraft lignin. [c] Determined by GC–FID analysis. [d] Reaction under basic conditions (pH 9).

Table 2 Activity and stereoselectivity of selected ADHs in the reduction of **2a** to **3a**[a]

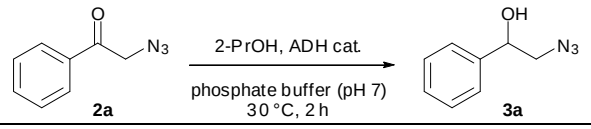

2a **3a**

Entry	Enzyme	Source / Supplier	Cofactor[b]	Conv.[c] [%]	Act.[d] [U/mg]	*ee*[e] [%]
1	ADH-A	*R. ruber*	NADH	12	0.5	>99 (*R*)
2	*Tb*ADH	*T. brockii*	NADPH	<1	<0.1	*nd*[f]
3	*Lk*ADH	*L. kefir*	NADPH	2	0.1	98 (*S*)
4	*Lb*ADH	*L. brevis*	NADPH	2	0.1	>99 (*S*)
5	KRED-NADH-110	Codexis	NADH	58	2.4	>99 (*S*)
6	KRED-P3-B03	Codexis	NADPH	5	0.2	>99 (*R*)
7	evo-1.1.030	evocatal	NADH	7	0.3	>99 (*R*)
8	evo-1.1.200	evocatal	NADH	73	3.1	>99 (*S*)

[a] Conditions: 50 mM **2a**, 0.1 mM NAD^+, 0.1 mg/mL ADH preparation, 5% (v/v) 2-PrOH, 30 °C, 2 h. For details, see Experimental Section. [b] Preferred cofactor according to literature or supplier's information. [c] Determined by GC–FID analysis. [d] Apparent activity [µmol product/(min · mg enzyme preparation)] calculated from conversion. [e] Enantiomeric excess of **3a** determined by chiral-phase GC–FID analysis. [f] *nd* = not determined.

A further selection was made according to the enzymes' tolerance for higher substrate concentrations and their operational stability. We identified ADH-A and KRED-NADH-110 as the most robust of the investigated Prelog- and anti-Prelog-selective enzymes, respectively, showing reasonable activity at 100 mM concentration of **2a** (Suppl. Fig. 1 and 2, ESI), and a good performance over 24 h of reaction time (Suppl. Fig. 3 and 4, ESI). The substrate scope of ADH-A and KRED-NADH-110 was investigated using the representative 2-azido-1-arylethanones **2a–f** as substrates. Both biocatalysts converted all six ketones tested with excellent stereoselectivity and with similar relative rates; only the reduction of **2f** by KRED-NADH-110 was surprisingly slow in comparison to the other 2-azido ketones (Fig. 2). Test transformations with 100 mM substrate concentration and optimised enzyme loadings (ADH-A: 1.5–2.5 mg/mL, KRED-NADH-110: 0.2–1.0 mg/mL; for details see ESI) proceeded to complete conversion within 20 h in all cases.

Chemo-enzymatic one-pot transformations

After suitable ADHs had been identified we proceeded with combining the enzymatic azido ketone reduction and Pd-NP-catalysed azide hydrogenation in a one-pot sequence. The biocatalytic reduction was run to completion (20 h) before adjusting the pH of the reaction mixture to 9 and adding a Pd-NP stock solution. First experiments showed that the activity of the nanoparticles was not impaired by the presence of the enzymes, and complete reduction of the intermediate azido alcohols **3a–f** was achieved in 4 h. However, in addition to the expected products **4**, the corresponding 2,2-dimethyloxazolidines **5** were also formed in minor amounts (4–10%), apparently by reaction of **4** with acetone generated as by-product in the ADH-catalysed reduction (Scheme 2).[24] When the bioreduction was carried out under reduced pressure, so as to remove the acetone from the solution, the one-pot sequence afforded essentially pure 1,2-amino alcohols **4a–f**. In semi-preparative-scale experiments (5 mL volume, 0.5 mmol substrate converted), the desired products could be isolated in good yield and excellent enantiomeric excess (Table 3). Only the isolated yields of **4f** fall behind compared to the other amino alcohols, which we attribute to the high aqueous solubility and the resulting difficult extraction of **4f**.

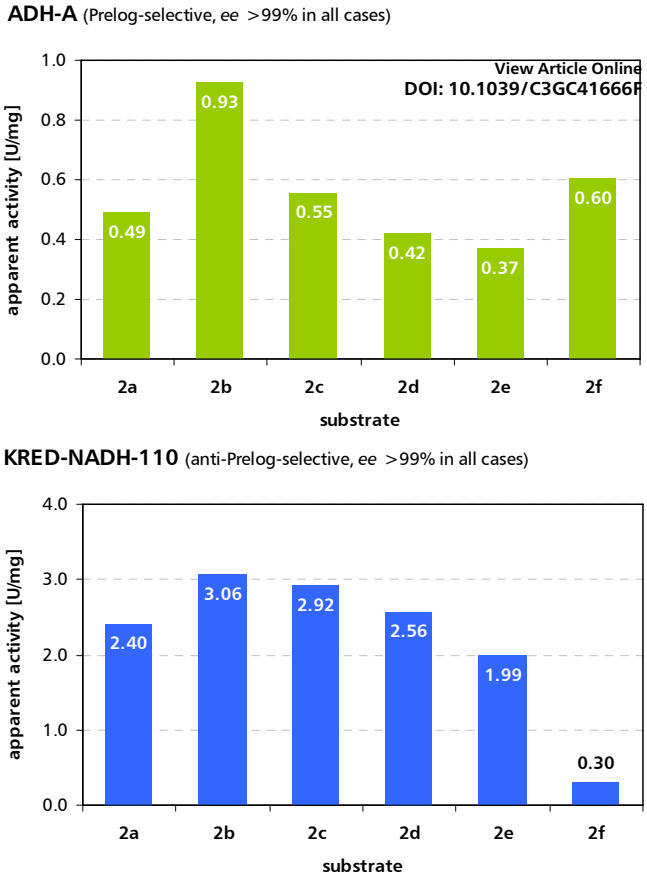

Fig. 2 Activity of ADH-A and KRED-NADH-110 in the reduction of azido ketones **2a–f**. Apparent activity [µmol product/(min · mg enzyme preparation)] determined from conversion after 2 h; conditions: 50 mM **2**, 0.1 mM NAD^+, 0.1 mg/mL ADH preparation, 5% (v/v) 2-PrOH, 30 °C. For details, see Experimental Section.

To further prove the preparative value and the scalability of the one-pot two-step reaction system we performed the conversion of azidoketone **2b** into 1,2-amino alcohol (*R*)-**4b** on gram scale (75 mL, 7.5 mmol substrate). ADH-A (1.5 mg/mL) was used as biocatalyst, and the target compound was isolated in 84% yield (1.08 g) and >99% *ee*.

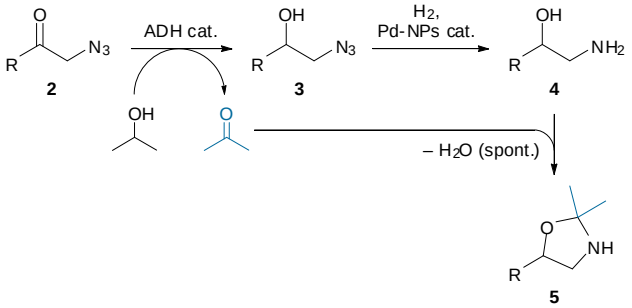

Scheme 2 Rationalisation of the formation of 2,2-dimethyloxazolidines **5** in the ADH/Pd-NP one-pot sequence

View Article Online
DOI: 10.1039/C3GC41666F

Table 3 Chemo-enzymatic two-step one-pot transformation of azido ketones **2a–f** into amino alcohols **4a–f**[a]

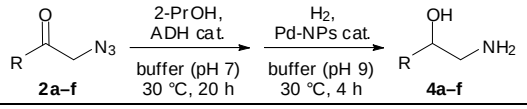

Entry	Subst.	ADH	GC yield (**4**)[b] [%]	Isol. yield (**4**)[c] [%]	*ee* (**4**)[d] [%]
1	**2a**	ADH-A	97	87 (60 mg)	>99 (*R*)
2	**2b**	ADH-A	98	89 (76 mg)	>99 (*R*)
3	**2c**	ADH-A	99	86 (67 mg)	>99 (*R*)
4	**2d**	ADH-A	99	85 (64 mg)	>99 (*R*)
5	**2e**	ADH-A	98	85 (71 mg)	>99 (*R*)
6	**2f**	ADH-A	>99	55 (35 mg)	>99 (*S*)[e]
7	**2a**	KRED-NADH-110	98	86 (59 mg)	>99 (*S*)
8	**2b**	KRED-NADH-110	98	78 (67 mg)	>99 (*S*)
9	**2c**	KRED-NADH-110	98	88 (68 mg)	>99 (*S*)
10	**2d**	KRED-NADH-110	98	86 (65 mg)	>99 (*S*)
11	**2e**	KRED-NADH-110	99	87 (73 mg)	>99 (*S*)
12	**2f**	KRED-NADH-110	>99	38 (24 mg)	>99 (*R*)[e]

[a] Conditions: 100 mM **2**, 0.1 mM NAD^+, 0.2–2.5 mg/mL ADH preparation, 0.5 mM Pd-NPs, 5% (v/v) 2-PrOH, 30 °C, 24 h. For details, see Experimental Section. [b] Relative amount of **4** in the crude product determined by GC–FID analysis. Rest to 100% is the corresponding 2,2-dimethyl-oxazolidine **5**. [c] Isolated yield of pure **4** after column chromatography; semi-preparative scale (5 mL; 0.5 mmol substrate). [d] Enantiomeric excess of **4** as determined by chiral GC–FID analysis after conversion into the corresponding 2,2-dimethyloxazolidine **5**. [e] Switch in substituent priorities according to Cahn–Ingold–Prelog rules.

Table 4 Chemo-enzymatic three-step one-pot transformation of halo ketones **1a–f** into amino alcohols **4a–f**[a]

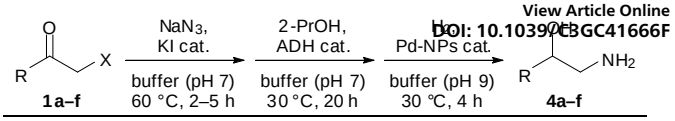

Entry	Subst.	ADH	GC yield (**4**)[b] [%]	Isol. yield (**4**)[c] [%]	*ee* (**4**)[d] [%]
1	**1a**	ADH-A	>99	83 (57 mg)	>99 (*R*)
2	**1b**	ADH-A	>99	75 (63 mg)	>99 (*R*)
3	**1c**	ADH-A	>99	89 (69 mg)	>99 (*R*)
4	**1d**	ADH-A	>99	81 (61 mg)	>99 (*R*)
5	**1e**	ADH-A	>99	75 (63 mg)	>99 (*R*)
6	**1f**	ADH-A	>99	39 (25 mg)	>99 (*S*)[e]
7	**1a**	KRED-NADH-110	99	76 (52 mg)	>99 (*S*)
8	**1b**	KRED-NADH-110	>99	80 (69 mg)	>99 (*S*)
9	**1c**	KRED-NADH-110	>99	79 (61 mg)	>99 (*S*)
10	**1d**	KRED-NADH-110	>99	82 (62 mg)	>99 (*S*)
11	**1e**	KRED-NADH-110	>99	86 (72 mg)	>99 (*S*)
12	**1f**	KRED-NADH-110	>99	36 (23 mg)	>99 (*R*)[e]

[a] Conditions: 100 mM **1**, 120 mM NaN_3, 10 mM KI, 0.1 mM NAD^+, 0.3–4.0 mg/mL ADH preparation, 0.5 mM Pd-NPs, 5% (v/v) 2-PrOH, 60–30 °C, 26–29 h. For details, see Experimental Section. [b] Relative amount of **4** in the crude product determined by GC–FID analysis. Rest to 100% is the corresponding 2,2-dimethyloxazolidine **5**. [c] Isolated yield of pure **4** after column chromatography; semi-preparative scale (5 mL; 0.5 mmol substrate). [d] Enantiomeric excess of **4** as determined by chiral GC–FID analysis after conversion into the corresponding 2,2-dimethyloxazolidine **5**. [e] Switch in substituent priorities according to Cahn–Ingold–Prelog rules.

Encouraged by the positive results of the ADH/Pd-NP combination, we sought to integrate the *in situ* formation of azido ketones **2** from the corresponding halo ketones **1** into the one-pot system. As a first test, **1a** was reacted at 60 °C with 1.2 equiv. of NaN_3 in buffer containing 5% (v/v) 2-propanol and varied amounts of potassium iodide as nucleophilic substitution catalyst. With 5 and 10 mol% of iodide, the reaction proceeded almost equally fast, and 90% of conversion was achieved within 4 h (Suppl. Fig. 5, ESI). Transferring the same conditions (10 mol% KI) to the autoclave setup used for the one-pot sequence, the azidolysis reaction of **1a–e** proceeded to completion within 5 h, while the furan derivative **1f** only required 2 h for full conversion. In addition, we found that the ADH-catalysed reduction could be performed on the crude reaction mixture of the azidolysis step, as a minor decrease in enzyme activity was easily compensated by slightly raising the enzyme loading. Hence, the sequential combination of all three reactions (azidolysis, ADH reduction, and hydrogenation) proved feasible. All steps of the one-pot process could be run to complete conversion, and no accumulation of any side products was observed. Consequently, the 1,2-amino alcohols **4a–f** were obtained with the same level of chemical and enantiomeric purity as in the two-step process (see Table 4).

An exemplary gram-scale conversion (75 mL, 7.5 mmol substrate) of **1c** into (*R*)-**4c** using ADH-A (2.0 mg/mL) as biocatalyst provided the 1,2-amino alcohol in 84% isolated yield (0.97 g) and optically pure form (*ee* >99%).

Finally, we wanted to apply our newly developed chemo-enzymatic one-pot reaction system to the asymmetric synthesis of a biologically active molecule. As target compound we chose (*S*)-tembamide, a naturally occurring benzamide derivative, for which antiviral (HIV) activity has been reported.[25] The synthesis required benzoylation of amino alcohol (*S*)-**4e** as the final step, which was achieved by simply adding a solution of benzoyl chloride (1.2 eq.) in MTBE to the alkaline, aqueous reaction mixture obtained after the Pd-NP-catalysed hydrogenation step (Scheme 3). A gram-scale reaction (50 mL, 5.0 mmol substrate, 0.5 mg/mL KRED-NADH-110 as biocatalyst) yielded 0.98 g (73% from **1e**) of (+)-(*S*)-tembamide, thus providing access to this natural product in a four-step one-pot operation.

Environmental impact assessment

Because of its highly 'integrative' nature we considered the tembamide synthesis a suitable test case for assessing the ecological benefits of the multi-step one-pot concept. Therefore, we performed a basic environmental impact analysis, in which we compared our four-step one-pot preparation of tembamide to previously reported asymmetric syntheses of this compound. We chose Sheldon's E-factor[26] (mass of waste produced per mass of desired product) as a simple metric. We also decided to exclude

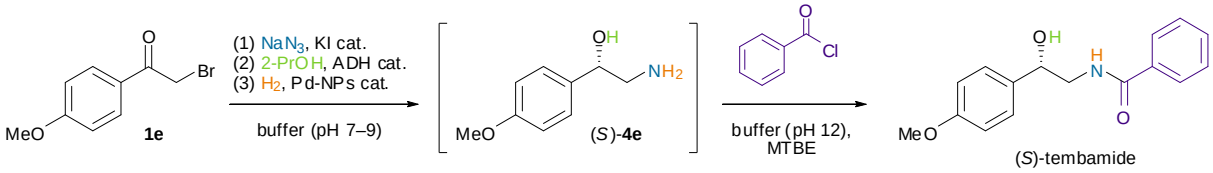

Scheme 3 Asymmetric synthesis of (*S*)-tembamide in a chemo-enzymatic four-step one-pot sequence

View Article Online
DOI: 10.1039/C3GC41666F

Table 5 Environmental impact comparison of catalytic asymmetric syntheses of tembamide

Article	Steps[a]	Asymmetric key step	Yield[b] [%]	E-factor[c]	Solvent[d] [mL/g]	Ref.
Present work	4 (1)	asymmetric ketone reduction (ADH)	73	11.1	309	–
Lee *et al.* 2007	5 (5)	asymmetric ketone reduction (Rh catalyst)	62	57.8	1600	27
Baeza *et al.* 2005	3 (2)	asymmetric cyano-*O*-phosphorylation (Lewis acid/Brønsted base catalyst)	65	23.3	1031	28
Kamal *et al.* 2004	5 (4)	enantioselective transesterification (lipase)	42	114.9	1801	29
Yadav *et al.* 2001	3 (2)[e]	asymmetric ketone reduction (carrot root)	85	97.5	826	16b
Brown *et al.* 1993, 1994	3 (3)	asymmetric hydrocyanation (peptide catalyst)	72	14.6	483	30

[a] Total number of chemical transformations. The number of steps carried out individually (with product isolation) is given in parentheses. [b] Overall yield. [c] Overall E-factor (excluding solvents). [d] Overall solvent demand. [e] Please note that this synthesis starts from 2-azido ketone **2e**, which is not commercially available, and therefore also needs to be synthesised.

solvents from the E-factor analysis and calculate the solvent demand as a second, independent indicator, since solvent waste and non-volatile waste (particularly salts) require very different processing. Both metrics can only provide a rough estimation of environmental impact, as they do not take into account the chemical composition (and hence the toxicity) of the waste, the energy demand of the involved processes, or the waste generated in the preparation of starting materials and catalysts. On the other hand, such a basic analysis is easily performed, and can thus serve as a quick eco-assessment of several synthetic options.

Table 5 provides an overview of the environmental performance of the six synthetic sequences under investigation. The chemo-enzymatic four-step one-pot system presented herein achieves the second-highest yield and has clear environmental advantages over the previously published procedures. Only the synthesis developed by Brown *et al.* reaches comparable values for yield, E-factor and solvent demand; however, it requires highly toxic hydrogen cyanide as a reagent in the asymmetric key step.

Differentiation of the E-factor into the contributions of the reaction itself (excess of reagents, coupled products, by-products, catalysts) and the down-stream processing reveals the main advantage of the one-pot concept: The elimination of isolation and purification steps leads to significant reductions in waste generation, which for all syntheses except the one reported by Yadav *et al.* (which uses large quantities of carrot root as a catalyst) is mainly linked to work-up and purification rather than loss of material in the reaction itself (Fig. 3). Nevertheless, our synthesis also features the lowest reaction-linked E-factor contribution (3.2) of the six procedures analysed.

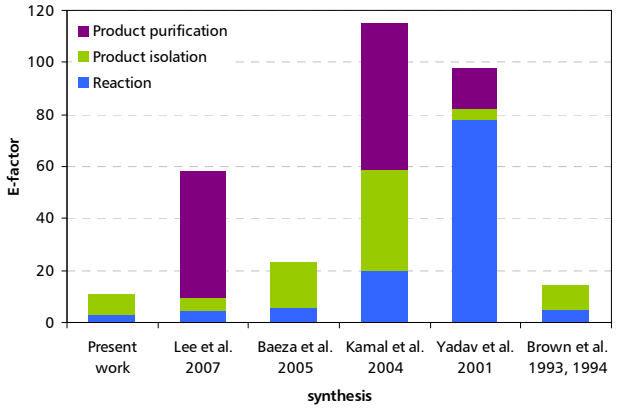

Fig. 3 Contributions of reaction steps, product isolation steps, and product purification steps to the overall E-factor (excluding solvents) of catalytic asymmetric syntheses of tembamide.

Differentiation by the type of waste (see Suppl. Fig. 10, ESI) shows that silica gel contributes substantially to the E-factor of the syntheses that make use of it. Those sequences that do not require chromatographic purifications (Baeza *et al.*, Brown *et al.*, and the present work), mainly produce inorganic salts (NaBr, NaCl, NaOH, Na_2SO_4, $MgSO_4$, and others) as waste, which are arguably less problematic.

Finally, a more detailed analysis of the different types of solvents used (see Suppl. Table 7, ESI) shows that our chemo-enzymatic sequence generally employs more environmentally acceptable solvents[31] (mostly water, ethyl acetate, and ethanol) than the other processes, especially because it avoids the use of chlorinated solvents and does not require eluents for chromatography, which often contain large amounts of hexane.

Conclusions

In summary, we have developed chemo-enzymatic one-pot reaction sequences that provide access to enantiomerically pure 1,2-amino alcohols either in two steps from the corresponding 2-azido ketones or in three steps from 2-halo ketones. The biocatalytic reduction of 2-azido ketones using alcohol dehydrogenases (ADHs) is the asymmetric key step in these processes, and by selecting suitable ADHs both enantiomers of the target compounds can be obtained in excellent enantiomeric excess (*ee* >99%). The 2-amino-1-arylethanol derivatives **4a–f** thus prepared are important building blocks in pharmaceutical research, for instance in the synthesis of anti-inflammatory, anti-viral, or anti-tumour agents.[32]

Furthermore, the one-pot concept has been applied to the asymmetric synthesis of the antiviral natural product (*S*)-tembamide, obtained in 73% yield over four steps and >99% *ee* from commercially available bromo ketone **1e**. This synthesis reaches high catalyst turnover (TON = 200 for Pd, 1000 for NAD^+, several 10,000 for the ADH),[33] uses only a small excess of reagents (1.2 eq. of NaN_3 and BzCl), and affords a chemically pure product after a final recrystallisation as the sole purification step. Due to these features, our method compares favourably with previous syntheses of tembamide not only in terms of yield, but especially regarding its ecological impact, as quantified by E-factor and solvent demand. Hence, our study highlights the advantages of chemo-enzymatic one-pot processes in the multi-step synthesis of chiral compounds, and since it uses catalysts that are either commercially available or easily prepared, we believe that it will also be of practical value to synthetic chemists.

Experimental

General Materials and Methods

Unless otherwise noted, reagents and organic solvents were obtained from chemical suppliers in reagent grade quality and used without further purification. Petroleum ether (boiling range 40–60 °C) and ethyl acetate used for extraction and column chromatography were purchased in technical grade quality and were distilled prior to use. *Pro analysi* (*p.a.*, >99% purity) grade solvents were used for handling the 1,2-amino alcohols **4a–f** to avoid any undesired oxazolidine formation due to contaminating acetone. Sulfonated lignin with either calcium or ammonium counterions was obtained from *Burgo Group S.p.A.*, Tolmezzo, Italy. Low-sulfonate Kraft lignin was obtained from *Sigma-Aldrich*. The halo ketones **1a–e** as well as both enantiomers of amino alcohol **4a** were obtained commercially; all other substrates and reference compounds were synthesised as described in the ESI.

The proprietary enzymes used in this study are part of the *Codexis* Codex KRED screening kit, the *Almac* selectAZyme CRED screening kit, and the *evocatal* ADH screening kit. The ADHs from *Lactobacillus kefir* and *Thermoanaerobium brockii* were obtained from *Sigma-Aldrich*. ADH-A from *Rhodococcus ruber* DSM 44541 and *Lb*ADH from *Lactobacillus brevis* were heterologously expressed in *E. coli* as described in the ESI.

Hydrogenation reactions, as well as analytical-scale (2 mL) and semi-preparative scale (5 mL) chemo-enzymatic one-pot transformations were carried out in magnetically stirred stainless steel autoclaves (16 mL total volume) that are part of a *HEL* PolyBlock8 parallel reactor system, and reactor temperature as well as stirring speed were controlled using the associated *HEL* WinISO software (v. 2.3.85.1). Gram-scale chemo-enzymatic one-pot transformations were carried out in a mechanically stirred *Parr* 4560 series stainless steel autoclave (452HC2 bomb cylinder, 160 mL total volume), and reactor temperature was controlled using a *Parr* 4841 heater/controller. Non-enzymatic reactions were generally stirred at 500 rpm, while biotransformations were stirred at 300 rpm (to minimise mechanical stress).

Thin layer chromatography was carried out on silica gel 60 F_{254} plates (*Merck*) and compounds were visualized either by UV or by dipping into cerium ammonium molybdate stain [50 g/L $(NH_4)_6Mo_7O_{24} \cdot 4\ H_2O$, 2 g/L $Ce(SO_4)_2 \cdot 4\ H_2O$ in 10% (v/v) sulfuric acid] or basic permanganate stain (50 g/L Na_2CO_3, 10 g/L $KMnO_4$, 0.85 g/L NaOH in demineralised water). Melting points were determined in open capillary tubes on a *Büchi* B-540 apparatus and are uncorrected. ^{1}H-NMR and ^{13}C-NMR spectra were recorded in $CDCl_3$ solution on a *Bruker* Avance 400 instrument at 400 and 100 MHz, respectively. Chemical shifts are given in parts per million (ppm) relative to the residual $CHCl_3$ peak (^{1}H: δ = 7.26 ppm, ^{13}C: δ = 77.2 ppm) and coupling constants (*J*) are reported in Hertz (Hz). Specific optical rotation values $[\alpha]_D^{20}$ were determined on a *Perkin-Elmer* Model 343 Polarimeter at 20 °C and a wavelength of 589 nm (sodium D-line) using a cuvette of 1 dm path length.

Azido alcohol hydrogenation catalysed by metal nanoparticles

Screening of metal nanoparticles for activity and selectivity in the hydrogenation of azido alcohol 3a: In a small-scale autoclave reactor (16 mL), 2-azido-1-phenylethanol (**3a**; 32 mg, 200 µmol; final conc. 100 mM) was dissolved in 2-propanol (100 µL; final conc. 5% v/v). Potassium phosphate buffer (1.7 mL, depending on nanoparticle type; 100 mM, pH 7.0, 1 mM $MgSO_4$) and a stock solution of metal nanoparticles in water (Pd: 180 µL of a 5.6 mM stock, Pt: 83 µL of a 12 mM stock; final conc. 0.5 mM) were added, and the mixture was stirred at 30 °C and 500 rpm under hydrogen atmosphere (10 bar) for 4 h. The reaction mixture was extracted with EtOAc (800 µL), the extract was dried over $MgSO_4$ and conversion was determined by GC–FID analysis.

Investigation of the tolerance of Pd nanoparticles towards the presence of ADHs and NAD(P)$^+$: Reactions were set up as described above, but contained 0.1–1.5 mg/mL of different ADHs and 100 µM NAD^+ or $NADP^+$.

Hydrogenation of azido alcohols 3a–f catalysed by Pd nanoparticles: Reactions were set up as described above, using 200 µmol (final conc. 100 mM) of azido alcohols **3a–f** as substrates. After 4 h, the reaction mixture was transferred to microcentrifuge tubes, the product was extracted into EtOAc (2 × 1 mL), and the extract was dried over $MgSO_4$. Evaporation of the solvent under reduced pressure afforded the crude amino alcohols **4a–f**. The conversion as well as the purity of the crude products were determined by GC–FID and NMR analysis.

Biotransformations

Screening of ADHs for activity and stereoselectivity in the reduction of azido ketone 2a: In a microcentrifuge tube (2 mL), 2-azidoacetophenone (**2a**; 4 mg, 25 µmol; final conc. 50 mM) was dissolved in 2-propanol (25 µL; final conc. 5% v/v, approx. 650 mM). Potassium phosphate buffer (425 µL; 100 mM, pH 7.0, 1 mM $MgSO_4$) and a stock solution of ADH (1 mg/mL; final conc. 0.1 mg/mL) and NAD(P)$^+$ (0.7 mg/mL, 1 mM; final conc. 100 µM) in potassium phosphate buffer (50 µL) were added, and the mixture was shaken at 30 °C and 1,000 rpm on a thermoshaker for 2 h. The reaction mixture was extracted with EtOAc (800 µL), the extract was dried over $MgSO_4$ and conversion as well as product *ee* were determined by GC–FID analysis.

Investigation of the substrate scope of ADH-A and KRED-NADH-110: In a microcentrifuge tube (2 mL), azido ketone **2a–f** (25 µmol; final conc. 50 mM) was dissolved in 2-propanol (25 µL; final conc. 5% v/v, approx. 650 mM). Potassium phosphate buffer (425 µL; 100 mM, pH 7.0, 1 mM $MgSO_4$) and a stock solution of ADH (1 mg/mL; final conc. 0.1 mg/mL) and NAD(P)$^+$ (0.7 mg/mL, 1 mM; final conc. 100 µM) in potassium phosphate buffer (50 µL) were added, and the mixture was shaken at 30 °C and 1,000 rpm on a thermoshaker for 2 h. The reaction mixture was extracted with EtOAc (800 µL), and the extract was dried over $MgSO_4$. Conversion was determined by GC–FID analysis, while product *ee* was determined either by GC–FID analysis (**3a**, **3e**, **3f**) or by HPLC analysis (**3b–d**).

Test transformations to ensure complete conversion under the conditions of the one-pot sequence were carried out in small-scale autoclave reactors (16 mL): Azido ketone **2a–f** (200 µmol; final conc. 100 mM) was dissolved/dispersed in 2-propanol (100 µL; final conc. 5% v/v, approx. 650 mM). Potassium phosphate buffer (1.7 mL; 100 mM, pH 7.0, 1 mM $MgSO_4$) and a stock solution of ADH (2–25 mg/mL; final conc. 0.2–2.5 mg/mL, see

Table 6) and NAD(P)$^+$ (0.7 mg/mL, 1 mM; final conc. 100 µM) in potassium phosphate buffer (200 µL) were added, and the mixture was stirred at 30 °C and 300 rpm for 20 h. The reaction mixture was transferred to microcentrifuge tubes, the product was extracted into EtOAc (2 × 1 mL), and the extract was dried over $MgSO_4$. Conversion was determined by GC–FID analysis, while product *ee* was determined by GC–FID analysis (**3a**, **3f**) or HPLC analysis (**3b–e**).

Chemo-enzymatic one-pot transformations

One-pot, two-step transformation of azido ketones 2a–f into amino alcohols 4a–f (analytical scale, 2 mL): A small-scale autoclave reactor (16 mL) was charged with the azido ketone **2** (200 µmol; final conc. 100 mM), 2-propanol (100 µL; final conc. 5% v/v, approx. 650 mM), potassium phosphate buffer (1.7 mL; 100 mM, pH 7.0, 1 mM $MgSO_4$) and a stock solution of ADH (ADH-A: 15–25 mg/mL, final conc. 1.5–2.5 mg/mL; *Codexis* KRED-NADH-110: 4.0–10 mg/mL, final conc. 0.4–1.0 mg/mL; see Table 6) and NAD$^+$ (0.7 mg/mL, 1 mM; final conc. 100 µM) in potassium phosphate buffer (200 µL), and the mixture was stirred at 30 °C and 300 rpm. The vent valve of the autoclave reactor was connected to a vacuum pump *via* a pressure control valve, and the reactor was evacuated to 200 mbar. After a reaction time of 18 h, the temperature was raised to 45 °C (to increase acetone evaporation) and stirring was continued for 2 h. A sample (50 µL) was taken, extracted with EtOAc (800 µL), the extract was dried over $MgSO_4$ and conversion was determined by GC analysis. The reaction mixture was then made alkaline (pH 9) by addition of 4 M aq. NaOH solution (25 µL), a stock solution of Pd nanoparticles (180 µL of a 5.6 mM stock; final conc. 0.5 mM) was added, and the mixture was stirred for another 4 h at 30 °C and 500 rpm under hydrogen atmosphere (10 bar). The reaction mixture was extracted with EtOAc (800 µL), the extract was dried over $MgSO_4$ and conversion as well as product *ee* were determined by GC analysis.

One-pot, two-step transformation of azido ketones 2a–f into amino alcohols 4a–f (semi-preparative scale, 5 mL): A small-scale autoclave reactor (16 mL) was charged with the azidoketone **2** (500 µmol; final conc. 100 mM), 2-propanol (250 µL; final conc. 5% v/v), potassium phosphate buffer (4.25 mL; 100 mM, pH 7.0, 1 mM $MgSO_4$) and a stock solution of ADH (ADH-A: 15–25 mg/mL, final conc. 1.5–2.5 mg/mL; *Codexis* KRED-NADH-110: 4.0–10 mg/mL, final conc. 0.4–1.0 mg/mL; see Table 6) and NAD$^+$ (0.7 mg/mL, 1 mM; final conc. 100 µM) in potassium phosphate buffer (500 µL), and the mixture was stirred at 30 °C and 300 rpm. The vent valve of the autoclave reactor was connected to a vacuum pump *via* a pressure control valve, and the reactor was evacuated to 200 mbar. After a reaction time of 18 h, the temperature was raised to 45 °C (to increase acetone evaporation) and stirring was continued for 2 h. The reaction mixture was then made alkaline (pH 9) by addition of 4 M aq. NaOH solution (65 µL), a stock solution of Pd nanoparticles (450 µL of a 5.6 mM stock; final conc. 0.5 mM) was added, and the mixture was stirred for an additional 4 h at 30 °C and 500 rpm under hydrogen atmosphere (10 bar). The reactor was depressurised, 4 M aq. NaOH solution (500 µL) was added, and the reaction mixture was saturated with NaCl. The product was extracted into EtOAc (4 × 5 mL), the combined extracts were dried over $MgSO_4$ and evaporated under reduced pressure to give the crude amino alcohols as orange oils or solids. Column chromatography (~0.6 g of silica gel 60 in a Pasteur pipette; MTBE → MTBE/MeOH/NH_4OH = 90/9/1) afforded the pure amino alcohols **4a–f**.

(*R*)-2-Amino-1-phenylethanol [(*R*)-4a]. 60 mg (87%) off-white solid. mp: 63–64 °C (lit.[34] 57–59 °C). TLC (silica, MTBE/MeOH/NH_4OH = 90/9/1): R_f = 0.10. $[\alpha]_D^{20}$ = –58.8 ($CHCl_3$, *c* = 1.31); lit.[35] (*S*) +60.6 ($CHCl_3$, *c* = 0.5). ^{1}H-NMR (400 MHz, $CDCl_3$): δ [ppm] = 2.25 (3H, br s, OH, NH_2), 2.80 (1H, dd, *J* = 12.8 Hz, 7.7 Hz, CH_2), 2.93 (1H, dd, *J* = 12.9 Hz, 3.9 Hz, CH_2), 4.62 (1H, dd, J = 7.8 Hz, 4.0 Hz, C*H*-OH), 7.26–7.37 (5H, m, Ar). ^{13}C-NMR (100 MHz, $CDCl_3$): δ [ppm] = 49.3, 74.4, 125.9, 127.5, 128.4, 142.6. GC–MS (EI, 70 eV): *m*/*z* = 137 (M$^+$, <1), 118 (3), 107 (31), 91 (11), 79 (100), 77 (79), 65 (6), 51 (37). The NMR data are in accordance with literature values.[36]

(*S*)-2-Amino-1-phenylethanol [(*S*)-4a]. 59 mg (86%) off-white solid. mp: 61–62 °C (lit.[34] 57–59 °C). TLC (silica, MTBE/MeOH/NH_4OH = 90/9/1): R_f = 0.10. $[\alpha]_D^{20}$ = +58.5 ($CHCl_3$, *c* = 1.53); lit.[35] +60.6 ($CHCl_3$, *c* = 0.5). NMR and MS data were in accordance with those of the opposite enantiomer.

(*R*)-2-Amino-1-(4-chlorophenyl)ethanol [(*R*)-4b]. 76 mg (89%) off-white solid. mp: 94–95 °C (lit.[37] 92–94 °C). TLC (silica, MTBE/MeOH/NH_4OH = 90/9/1): R_f = 0.11. $[\alpha]_D^{20}$ = –64.5 ($CHCl_3$, *c* = 1.08); lit.[38] (*S*) +67.4 ($CHCl_3$, *c* = 0.35). ^{1}H-NMR (400 MHz, $CDCl_3$): δ [ppm] = 2.30 (3H, br s, OH, NH_2), 2.73 (1H, dd, *J* = 12.8 Hz, 7.8 Hz, CH_2), 2.92 (1H, d, *J* = 11.3 Hz, CH_2), 4.57 (1H, dd, J = 8.0 Hz, 3.9 Hz, C*H*-OH), 7.26 (2H, d, *J* = 8.3 Hz, Ar-*o*), 7.31 (2H, d, *J* = 8.1 Hz, Ar-*m*). ^{13}C-NMR (100 MHz, $CDCl_3$): δ [ppm] = 49.2, 73.5, 127.2, 128.5, 133.1, 141.1. GC–MS (EI, 70 eV): *m*/*z* = 171 (M$^+$, 1), 143 (5), 141 (16), 115 (4), 113 (13), 77 (100), 51 (28), 50 (14). The NMR data are in accordance with literature values.[36]

(*S*)-2-Amino-1-(4-chlorophenyl)ethanol [(*S*)-4b]. 67 mg (78%) off-white solid. mp: 94–95 °C (lit.[37] 92–94 °C). TLC (silica, MTBE/MeOH/NH_4OH = 90/9/1): R_f = 0.11. $[\alpha]_D^{20}$ = +64.7 ($CHCl_3$, *c* = 0.71); lit.[38] +67.4 ($CHCl_3$, *c* = 0.35). NMR and MS data were in accordance with those of the opposite enantiomer.

(*R*)-2-Amino-1-(4-fluorophenyl)ethanol [(*R*)-4c]. 67 mg (86%) off-white solid. mp: 83–84 °C (lit.[38] 63–65 °C). TLC (silica, MTBE/MeOH/NH_4OH = 90/9/1): R_f = 0.10. $[\alpha]_D^{20}$ = –66.8 ($CHCl_3$, *c* = 1.08); lit.[38] (*S*) +40.8 (EtOH, *c* = 1.68). ^{1}H-NMR (400 MHz, $CDCl_3$): δ [ppm] = 2.24 (3H, br s, OH, NH_2), 2.75 (1H, dd, *J* = 12.8 Hz, 7.9 Hz, CH_2), 2.94 (1H, dd, *J* = 12.6 Hz, 3.9 Hz, CH_2), 4.59 (1H, dd, *J* = 8.0 Hz, 3.9 Hz, C*H*-OH), 7.03 (2H, t, *J* = 8.5 Hz, Ar-*m*), 7.31 (2H, dd, *J* = 8.3 Hz, 5.4 Hz, Ar-*o*). ^{13}C-NMR (100 MHz, $CDCl_3$): δ [ppm] = 49.3, 73.6, 115.2 (d, J_{CF} = 21.3 Hz), 127.5 (d, J_{CF} = 8.0 Hz), 138.3 (d, J_{CF} = 3.1 Hz), 162.2 (d, J_{CF} = 245 Hz). GC–MS (EI, 70 eV): *m*/*z* = 155 (M$^+$, 1), 125 (39), 123 (16), 109 (14), 97 (100), 95 (41), 77 (56), 75 (22), 70 (8), 57 (11), 51 (25), 50 (14). The NMR data are in accordance with literature values.[38]

(*S*)-2-Amino-1-(4-fluorophenyl)ethanol [(*S*)-4c]. 68 mg (88%) off-white solid. mp: 83–84 °C (lit.[38] 63–65 °C). TLC (silica, MTBE/MeOH/NH_4OH = 90/9/1): R_f = 0.10. $[\alpha]_D^{20}$ = +66.7 ($CHCl_3$, *c* = 0.90); lit.[38] +40.8 (EtOH, *c* = 1.68). NMR and MS data were in accordance with those of the opposite enantiomer.

View Article Online
DOI: 10.1039/C3GC41666F

(*R*)-2-Amino-1-(4-tolyl)ethanol [(*R*)-4d]. 64 mg (85%) off-white solid. mp: 59–60 °C (lit.[37] 67–69 °C). TLC (silica, MTBE/MeOH/NH_4OH = 90/9/1): R_f = 0.11. $[\alpha]_D^{20}$ = –65.5 ($CHCl_3$, *c* = 1.00); lit.[39] –32 ($CHCl_3$, *c* = 5.0). ^{1}H-NMR (400 MHz, $CDCl_3$): δ [ppm] = 2.19 (3H, br s, OH, NH_2), 2.35 (3H, s CH_3), 2.79 (1H, dd, *J* = 12.8 Hz, 7.8 Hz, CH_2), 2.93 (1H, d, *J* = 11.1 Hz, CH_2), 4.58 (1H, dd, *J* = 7.8 Hz, 4.0 Hz, C*H*-OH), 7.16 (2H, d, *J* = 7.7 Hz, Ar-*m*), 7.23 (2H, d, *J* = 7.6 Hz, Ar-*o*). ^{13}C-NMR (100 MHz, $CDCl_3$): δ [ppm] = 21.1, 49.3, 74.3, 125.8, 129.1, 137.1, 139.7. GC–MS (EI, 70 eV): *m*/*z* = 151 (M^+, 3), 122 (15), 121 (100), 119 (12), 93 (93), 91 (96), 77 (75), 65 (28), 51 (18). The NMR data are in accordance with literature values.[10d]

(*S*)-2-Amino-1-(4-tolyl)ethanol [(*S*)-4d; CAS 149403-05-4]. 65 mg (86%) off-white solid. mp: 59–60 °C (lit.[37] 67–69 °C). TLC (silica, MTBE/MeOH/NH_4OH = 90/9/1): R_f = 0.11. $[\alpha]_D^{20}$ = +65 ($CHCl_3$, *c* = 1.00); lit. (*R*)[39] –32 ($CHCl_3$, *c* = 5.0). NMR and MS data were in accordance with those of the opposite enantiomer.

(*R*)-2-Amino-1-(4-methoxyphenyl)ethanol [(*R*)-4e]. 71 mg (85%) off-white solid. mp: 102–103 °C. TLC (silica, MTBE/MeOH/NH_4OH = 90/9/1): R_f = 0.09. $[\alpha]_D^{20}$ = –61.4 ($CHCl_3$, *c* = 0.93); lit.[38] –39.9 ($CHCl_3$, *c* = 1.03). ^{1}H-NMR (400 MHz, $CDCl_3$): δ [ppm] = 1.94 (3H, br s, OH, NH_2), 2.79 (1H, dd, *J* = 12.8 Hz, 7.8 Hz, CH_2), 2.97 (1H, dd, *J* = 12.5 Hz, 4.0 Hz, CH_2), 3.81 (3H, s, OCH_3), 4.59 (1H, dd, *J* = 7.9 Hz, 4.1 Hz, C*H*-OH), 6.90 (2H, d, *J* = 8.7 Hz, Ar-*m*), 7.29 (2H, d, *J* = 8.8 Hz, Ar-*o*). ^{13}C-NMR (100 MHz, $CDCl_3$): δ [ppm] = 49.3, 55.3, 74.1, 113.8, 127.1, 134.6, 159.1. GC–MS (EI, 70 eV): *m*/*z* = 167 (M^+, 3), 138 (10), 137 (100), 109 (42), 94 (43), 77 (40), 66 (14), 65 (10), 51 (9). The NMR data are in accordance with literature values.[10d]

(*S*)-2-Amino-1-(4-methoxyphenyl)ethanol [(*S*)-4e; CAS 46084-19-9]. 73 mg (87%) off-white solid. mp: 102–103 °C. TLC (silica, MTBE/MeOH/NH_4OH = 90/9/1): R_f = 0.09. $[\alpha]_D^{20}$ = +61.6 ($CHCl_3$, *c* = 1.01); lit. (*R*)[38] –39.9 ($CHCl_3$, *c* = 1.03). NMR and MS data were in accordance with those of the opposite enantiomer.

(*S*)-2-Amino-1-(2-furyl)ethanol [(*S*)-4f]. 35 mg (55%) yellowish solid. mp: 80–81 °C. TLC (silica, MTBE/MeOH/NH_4OH = 90/9/1): R_f = 0.14. $[\alpha]_D^{20}$ = –33.5 ($CHCl_3$, *c* = 0.93); lit.[40] –38.6 ($CHCl_3$, *c* = 1.80). ^{1}H-NMR (400 MHz, $CDCl_3$): δ [ppm] = 2.53 (3H, br s, OH, NH_2), 2.98 (2H, d, *J* = 5.8 Hz, CH_2), 4.61 (1H, t, *J* = 5.8 Hz, C*H*-OH), 6.24 (1H, d, *J* = 3.3 Hz, Ar-3), 6.32 (1H, dd, *J* = 3.2 Hz, 1.8 Hz, Ar-4) 7.35 (1H, d, *J* = 1.8 Hz, Ar-5). ^{13}C-NMR (100 MHz, $CDCl_3$): δ [ppm] = 46.0, 68.2, 106.3, 110.2, 142.0, 155.5. GC–MS (EI, 70 eV): *m*/*z* = 127 (M^+, 12), 98 (82), 97 (86), 81 (8), 69 (33), 53 (17), 51 (15), 42 (24), 41 (100). The NMR data are in accordance with literature values.[41]

(*R*)-2-Amino-1-(2-furyl)ethanol [(*R*)-4f]. 24 mg (38%) yellowish solid. mp: 81–82 °C. TLC (silica, MTBE/MeOH/NH_4OH = 90/9/1): R_f = 0.14. $[\alpha]_D^{20}$ = +33.6 ($CHCl_3$, *c* = 0.85); lit. (*S*)[40] –38.6 ($CHCl_3$, *c* = 1.80). NMR and MS data were in accordance with those of the opposite enantiomer.

The ADH concentrations used for the one-pot, two-step transformation of azido ketones **2a–f** into amino alcohols **4a–f** are summarised in Table 6:

Table 6 ADH concentrations used for the two-step one-pot transformation of azido ketones **2a–f** into amino alcohols **4a–f**.

Substrate	*c*(ADH-A)[a] [mg/mL]	*c*(KRED-NADH-130)[a] [mg/mL]
2a	1.5	0.2
2b	1.5	0.2
2c	1.5	0.2
2d	1.5	0.2
2e	2.5	0.4
2f	1.5	1.0

[a] Final concentration of crude ADH preparation in the reaction mixture.

One-pot, two-step transformation of azido ketone 2b into amino alcohol (*R*)-4b (gram scale, 75 mL): An autoclave reactor (160 mL) was charged with 2-azido-4'-chloroacetophenone (**2b**; 1.47 g, 7.5 mmol; final conc. 100 mM), 2-propanol (3.75 mL; final conc. 5% v/v), potassium phosphate buffer (66.25 mL; 100 mM, pH 7.0, 1 mM $MgSO_4$) and a stock solution of ADH-A (113 mg; final conc. 1.5 mg/mL) and NAD^+ (6 mg; final conc. 100 µM) in potassium phosphate buffer (5 mL), and the mixture was stirred at 30 °C and 300 rpm. The vent valve of the autoclave reactor was connected to a vacuum pump *via* a pressure control valve, and the reactor was evacuated to 200 mbar. After a reaction time of 18 h, the temperature was raised to 45 °C and stirring continued for 2 h. The reaction mixture was cooled to room temperature, and complete consumption of the **2b** was verified by TLC analysis. The reaction mixture was then made alkaline (pH 9) by addition of 4 M aq. NaOH solution (1 mL), a stock solution of Pd nanoparticles (6.7 mL of a 5.6 mM stock; final conc. 0.5 mM) was added, and the mixture was stirred for an additional 16 h (overnight) at 30 °C and 500 rpm under hydrogen atmosphere (10 bar). Complete consumption of **3b** was verified by TLC analysis, 4 M aq. NaOH solution (10 mL) was added, and the reaction mixture was saturated with NaCl. The product was extracted into EtOAc (5 × 40 mL; phase separation accelerated by centrifugation), and the combined extracts were dried over $MgSO_4$ and evaporated under reduced pressure to give 1.30 g of an orange solid. Column chromatography (silica gel 60, MTBE → MTBE/MeOH/NH_4OH = 90/9/1) afforded 1.08 g (84%) of (*R*)-**4b** as an off-white solid. mp: 94–95 °C (lit.[37] 92–94 °C). TLC (silica, MTBE/MeOH/NH_4OH = 90/9/1): R_f = 0.11. $[\alpha]_D^{20}$ = –64.4 ($CHCl_3$, *c* = 0.94); lit.[38] (*S*) +67.4 ($CHCl_3$, *c* = 0.35). NMR and MS data were in accordance with those obtained for the product of the semi-preparative scale experiment.

One-pot, three-step transformation of halo ketones 1a–f into amino alcohols 4a–f (analytical scale, 2 mL): A small-scale autoclave reactor (16 mL) was charged with the halo ketone **1** (200 µmol; final conc. 100 mM), 2-propanol (100 µL; final conc. 5% v/v, approx. 650 mM) and potassium phosphate buffer (1.9 mL; 100 mM, pH 7.0, 1 mM $MgSO_4$) containing NaN_3 (7.8 mg/mL, 120 mM) and KI (1.7 mg/mL, 10 mM), and the mixture was stirred at 60 °C and 500 rpm for 2–5 h. A sample (50 µL) was taken, extracted with EtOAc (800 µL), the extract was dried over $MgSO_4$ and conversion was determined by GC analysis. Additional 2-propanol (100 µL; to supplement the material lost through evaporation) and a stock solution of ADH (ADH-A: 20–30 mg/mL, final conc. 2.0–3.0 mg/mL; *Codexis* KRED-NADH-110: 5.0–15 mg/mL, final conc. 0.5–1.5 mg/mL; see Table 7) and NAD^+ (0.7 mg/mL, 1 mM; final conc. 100 µM) in potassium

phosphate buffer (200 µL) were added, and the mixture was stirred at 30 °C and 300 rpm. The vent valve of the autoclave reactor was connected to a vacuum pump *via* a pressure control valve, and the reactor was evacuated to 200 mbar. After a reaction time of 18 h, the temperature was raised to 45 °C (to increase acetone evaporation) and stirring was continued for 2 h. A sample (50 µL) was taken, extracted with EtOAc (800 µL), the extract was dried over $MgSO_4$ and conversion was determined by GC analysis. The reaction mixture was then made alkaline (pH 9) by addition of 4 M aq. NaOH solution (25 µL), a stock solution of Pd nanoparticles (180 µL of a 5.6 mM stock; final conc. 0.5 mM) was added, and the mixture was stirred for another 4 h at 30 °C and 500 rpm under hydrogen atmosphere (10 bar). The reaction mixture was extracted with EtOAc (800 µL), the extract was dried over $MgSO_4$ and conversion as well as product *ee* were determined by GC analysis.

One-pot, three-step transformation of halo ketones 1a–f into amino alcohols 4a–f (semi-preparative scale, 5 mL): A small-scale autoclave reactor (16 mL) was charged with the halo ketone **1** (500 µmol; final conc. 100 mM), 2-propanol (250 µL; final conc. 5% v/v, approx. 650 mM) and potassium phosphate buffer (4.9 mL; 100 mM, pH 7.0, 1 mM $MgSO_4$) containing NaN_3 (7.8 mg/mL, 120 mM) and KI (1.7 mg/mL, 10 mM), and the mixture was stirred at 60 °C and 500 rpm for 2–5 h. After cooling to room temperature, any larger agglomerates of solid **2** were broken into smaller pieces using a stirring rod, additional 2-propanol (250 µL; to supplement the material lost through evaporation) and a stock solution of ADH (ADH-A: 20–35 mg/mL, final conc. 2.0–3.5 mg/mL; *Codexis* KRED-NADH-110: 5.0–15 mg/mL, final conc. 0.5–1.5 mg/mL; see Table 7) and NAD^+ (0.7 mg/mL, 1 mM; final conc. 100 µM) in potassium phosphate buffer (500 µL) were added, and the mixture was stirred at 30 °C and 300 rpm. The vent valve of the autoclave reactor was connected to a vacuum pump *via* a pressure control valve, and the reactor was evacuated to 200 mbar. After a reaction time of 18 h, the temperature was raised to 45 °C (to increase acetone evaporation) and stirring was continued for 2 h. The reaction mixture was then made alkaline (pH 9) by addition of 4 M aq. NaOH solution (65 µL), a stock solution of Pd nanoparticles (450 µL of a 5.6 mM stock; final conc. 0.5 mM) was added, and the mixture was stirred for an additional 4 h at 30 °C and 500 rpm under hydrogen atmosphere (10 bar). The reactor was depressurised, 4 M aq. NaOH solution (500 µL) was added, and the reaction mixture was saturated with NaCl. The product was extracted into EtOAc (4 × 5 mL), the combined extracts were dried over $MgSO_4$ and evaporated under reduced pressure to give the crude amino alcohols as orange oils or solids. Column chromatography (~0.6 g of silica gel 60 in a Pasteur pipette; MTBE → MTBE/MeOH/NH_4OH = 90/9/1) afforded the pure amino alcohols **4a–f**.

(*R*)-2-Amino-1-phenylethanol [(*R*)-4a]. 57 mg (83%) off-white solid. mp: 62–63 °C (lit.[34] 57–59 °C). TLC (silica, MTBE/MeOH/NH_4OH = 90/9/1): R_f = 0.10. $[\alpha]_D^{20}$ = –58.8 ($CHCl_3$, c = 1.31); lit. (*S*) [35] +60.6 ($CHCl_3$, c = 0.5). NMR and MS data were in accordance with those obtained for the product of the two-step one-pot sequence.

(*S*)-2-Amino-1-phenylethanol [(*S*)-4a]. 52 mg (76%) off-white solid. mp: 61–62 °C (lit.[34] 57–59 °C). TLC (silica, MTBE/MeOH/NH_4OH = 90/9/1): R_f = 0.10. $[\alpha]_D^{20}$ = +59.0 ($CHCl_3$, c = 1.02); lit.[35] +60.6 ($CHCl_3$, c = 0.5). NMR and MS data were in accordance with those obtained for the product of the two-step one-pot sequence.

View Article Online
DOI: 10.1039/C3GC41666F

(*R*)-2-Amino-1-(4-chlorophenyl)ethanol [(*R*)-4b]. 63 mg (75%) off-white solid. mp: 93–95 °C (lit.[37] 92–94 °C). TLC (silica, MTBE/MeOH/NH_4OH = 90/9/1): R_f = 0.11. $[\alpha]_D^{20}$ = –64.2 ($CHCl_3$, c = 1.08); lit. (*S*)[38] +67.4 ($CHCl_3$, c = 0.35). NMR and MS data were in accordance with those obtained for the product of the two-step one-pot sequence.

(*S*)-2-Amino-1-(4-chlorophenyl)ethanol [(*S*)-4b]. 69 mg (80%) off-white solid. mp: 94–95 °C (lit.[37] 92–94 °C). TLC (silica, MTBE/MeOH/NH_4OH = 90/9/1): R_f = 0.11. $[\alpha]_D^{20}$ = +64.4 ($CHCl_3$, c = 1.10); lit.[38] +67.4 ($CHCl_3$, c = 0.35). NMR and MS data were in accordance with those obtained for the product of the two-step one-pot sequence.

(*R*)-2-Amino-1-(4-fluorophenyl)ethanol [(*R*)-4c]. 69 mg (89%) off-white solid. mp: 82–83 °C (lit.[38] 63–65 °C). TLC (silica, MTBE/MeOH/NH_4OH = 90/9/1): R_f = 0.10. $[\alpha]_D^{20}$ = –66.9 ($CHCl_3$, c = 1.04); lit. (*S*)[38] +40.8 (EtOH, c = 1.68). NMR and MS data were in accordance with those obtained for the product of the two-step one-pot sequence.

(*S*)-2-Amino-1-(4-fluorophenyl)ethanol [(*S*)-4c]. 61 mg (79%) off-white solid. mp: 83–84 °C (lit.[38] 63–65 °C). TLC (silica, MTBE/MeOH/NH_4OH = 90/9/1): R_f = 0.10. $[\alpha]_D^{20}$ = +66.7 ($CHCl_3$, c = 1.04); lit.[38] +40.8 (EtOH, c = 1.68). NMR and MS data were in accordance with those obtained for the product of the two-step one-pot sequence.

(*R*)-2-Amino-1-(4-tolyl)ethanol [(*R*)-4d]. 64 mg (85%) off-white solid. mp: 56–58 °C (lit.[37] 67–69 °C). TLC (silica, MTBE/MeOH/NH_4OH = 90/9/1): R_f = 0.11. $[\alpha]_D^{20}$ = –64.5 ($CHCl_3$, c = 1.02); lit.[39] –32 ($CHCl_3$, c = 5.0). NMR and MS data were in accordance with those obtained for the product of the two-step one-pot sequence.

(*S*)-2-Amino-1-(4-tolyl)ethanol [(*S*)-4d]. 62 mg (82%) off-white solid. mp: 57–58 °C (lit.[37] 67–69 °C). TLC (silica, MTBE/MeOH/NH_4OH = 90/9/1): R_f = 0.11. $[\alpha]_D^{20}$ = +64.8 ($CHCl_3$, c = 1.00); lit. (*R*)[39] –32 ($CHCl_3$, c = 5.0). NMR and MS data were in accordance with those obtained for the product of the two-step one-pot sequence.

(*R*)-2-Amino-1-(4-methoxyphenyl)ethanol [(*R*)-4e]. 71 mg (85%) off-white solid. mp: 102–103 °C. TLC (silica, MTBE/MeOH/NH_4OH = 90/9/1): R_f = 0.09. $[\alpha]_D^{20}$ = –61.4 ($CHCl_3$, c = 0.93); lit.[38] –39.9 ($CHCl_3$, c = 1.03). NMR and MS data were in accordance with those obtained for the product of the two-step one-pot sequence.

(*S*)-2-Amino-1-(4-methoxyphenyl)ethanol [(*S*)-4e]. 72 mg (86%) off-white solid. mp: 103–104 °C. TLC (silica, MTBE/MeOH/NH_4OH = 90/9/1): R_f = 0.09. $[\alpha]_D^{20}$ = +61.4 ($CHCl_3$, c = 1.24); lit. (*R*)[38] –39.9 ($CHCl_3$, c = 1.03). NMR and MS data were in accordance with those obtained for the product of the two-step one-pot sequence.

(*S*)-2-Amino-1-(2-furyl)ethanol [(*S*)-4f]. 25 mg (39%) yellowish solid. mp: 79–81 °C. TLC (silica, MTBE/MeOH/NH_4OH = 90/9/1): R_f = 0.14. $[\alpha]_D^{20}$ = –33.9 ($CHCl_3$, c = 0.77); lit.[40] –38.6 ($CHCl_3$, c = 1.80). NMR and MS data were in accordance with those obtained for the product of the two-step one-pot sequence.

(*R*)-2-Amino-1-(2-furyl)ethanol [(*R*)-4f]. 23 mg (36%)

yellowish solid. mp: 80–81 °C. TLC (silica, MTBE/MeOH/NH_4OH = 90/9/1): R_f = 0.14. $[\alpha]_D^{20}$ = +33.8 ($CHCl_3$, *c* = 0.75); lit. (*S*)[40] –38.6 ($CHCl_3$, *c* = 1.80). NMR and MS data were in accordance with those obtained for the product of the two-step one-pot sequence.

The ADH concentrations used for the one-pot, three-step transformation of halo ketones **1a–f** into amino alcohols **4a–f** are summarised in Table 7:

Table 7 ADH concentrations used for the three-step one-pot transformation of halo ketones **1a–f** into amino alcohols **4a–f**.

Substrate	*c*(ADH-A)[a] [mg/mL]	*c*(KRED-NADH-110)[a] [mg/mL]
2a	2.0	0.3
2b	2.0	0.3
2c	2.0	0.3
2d	2.0	0.3
2e	3.0	0.5
2f	2.0	1.5

[a] Final concentration of crude ADH preparation in the reaction mixture.

One-pot, three-step transformation of halo ketone 1c into amino alcohols (*R*)-4c (gram scale, 75 mL): An autoclave reactor (160 mL) was charged with the 2-bromo-4'-fluoroacetophenone (**1c**; 1.63 g, 7.5 mmol; final conc. 100 mM), 2-propanol (3.75 mL; final conc. 5% v/v, approx. 650 mM) and potassium phosphate buffer (71.25 mL; 100 mM, pH 7.0, 1 mM $MgSO_4$) containing NaN_3 (0.59 g, 9 mmol; final conc. 120 mM) and KI (0.13 g, 0.75 mmol; final conc. 10 mM), and the mixture was stirred at 60 °C and 500 rpm for 5 h. The reaction mixture was cooled to room temperature, and complete consumption of **1c** was verified by TLC analysis. Any larger agglomerates of solid **2c** were broken into smaller pieces using a stirring rod, additional 2-propanol (3.75 mL; to supplement the material lost through evaporation) and a stock solution of ADH-A (150 mg; final conc. 2.0 mg/mL) and NAD^+ (5.3 mg; final conc. 100 µM) in potassium phosphate buffer (5 mL) were added, and the mixture was stirred at 30 °C and 300 rpm. The vent valve of the autoclave reactor was connected to a vacuum pump *via* a pressure control valve, and the reactor was evacuated to 200 mbar. After a reaction time of 18 h, the temperature was raised to 45 °C (to increase acetone evaporation) and stirring was continued for 2 h. The reaction mixture was cooled to room temperature, and complete consumption of **2c** was verified by TLC analysis. The reaction mixture was then made alkaline (pH 9) by addition of 4 M aq. NaOH solution (1 mL), a stock solution of Pd nanoparticles (6.7 mL of a 5.6 mM stock; final conc. 0.5 mM) was added, and the mixture was stirred for an additional 4 h at 30 °C and 500 rpm under hydrogen atmosphere (10 bar). Complete consumption of **3c** was verified by TLC analysis, 4 M aq. NaOH solution (10 mL) was added, and the reaction mixture was saturated with NaCl. The product was extracted into EtOAc (5 × 40 mL; phase separation accelerated by centrifugation), and the combined extracts were dried over $MgSO_4$ and evaporated under reduced pressure to give 1.06 g of an orange solid. Column chromatography (silica gel 60, MTBE → MTBE/MeOH/NH_4OH = 90/9/1) afforded 0.97 g (84%) of (*R*)-**4c** as an off-white solid. mp: 83–84 °C (lit.[38] 63–65 °C). TLC (silica, MTBE/MeOH/NH_4OH = 90/9/1): R_f = 0.10. $[\alpha]_D^{20}$ = –66.5 ($CHCl_3$, *c* = 0.92); lit. (*S*)[38] +40.8 (EtOH, *c* = 1.68). NMR and MS data were in accordance with those obtained for the product of the semi-preparative scale experiment.

One-pot, four-step transformation of halo ketone 1e into (*S*)-tembamide [CAS 15779-24-5] (gram scale, 50 mL): An autoclave reactor (160 mL) was charged with the 2-bromo-4'-methoxyacetophenone (**1e**; 1.15 g, 7.5 mmol; final conc. 100 mM), 2-propanol (2.5 mL; final conc. 5% v/v, approx. 650 mM) and potassium phosphate buffer (47.5 mL; 100 mM, pH 7.0, 1 mM $MgSO_4$) containing NaN_3 (0.39 g, 6 mmol; final conc. 120 mM) and KI (0.08 g, 0.5 mmol; final conc. 10 mM), and the mixture was stirred at 60 °C and 500 rpm for 5 h. The reaction mixture was cooled to room temperature, and complete consumption of **1e** was verified by TLC analysis. Any larger agglomerates of solid **2e** were broken into smaller pieces using a stirring rod, additional 2-propanol (2.5 mL; to supplement the material lost through evaporation) and a stock solution of *Codexis* KRED-NADH-110 (25 mg; final conc. 0.5 mg/mL) and NAD^+ (3.3 mg; final conc. 100 µM) in potassium phosphate buffer (5 mL) were added, and the mixture was stirred at 30 °C and 300 rpm. The vent valve of the autoclave reactor was connected to a vacuum pump *via* a pressure control valve, and the reactor was evacuated to 200 mbar. After a reaction time of 18 h, the temperature was raised to 45 °C (to increase acetone evaporation) and stirring was continued for 2 h. The reaction mixture was cooled to room temperature, and complete consumption of **2e** was verified by TLC analysis. The reaction mixture was then made alkaline (pH 9) by addition of 4 M aq. NaOH solution (1 mL), a stock solution of Pd nanoparticles (6.7 mL of a 5.6 mM stock; final conc. 0.5 mM) was added, and the mixture was stirred for an additional 4 h at 30 °C and 500 rpm under hydrogen atmosphere (10 bar). Complete consumption of **3e** was verified by TLC analysis, 4 M aq. NaOH solution (1.5 mL) and a solution of benzoyl chloride (0.84 g, 6.0 mmol) in MTBE (15 mL) were added, and stirring was continued at room temperature for 2 h. Complete consumption of **4e** was verified by TLC analysis, EtOAc (20 mL) was added, and the phases were separated (accelerated by centrifugation). The aqueous phase was extracted with EtOAc (3 × 30 mL; phase separation accelerated by centrifugation), the combined extracts were washed with 1 M aq. NaOH solution (40 mL) and brine (10 mL), and dried over $MgSO_4$. The solvent was evaporated under reduced pressure to give 1.40 g of an off-white solid. Recrystallisation (EtOH/water = 8/2) afforded 0.98 g (73%) of (*S*)-tembamide as a colourless, crystalline solid. mp: 148–149 °C (lit.[27] 145–147 °C). TLC (silica, MTBE/MeOH/NH_4OH = 90/9/1): R_f = 0.10. $[\alpha]_D^{20}$ = +54.9 ($CHCl_3$, *c* = 0.52); lit.[29] +56.9 ($CHCl_3$, *c* = 0.54). ^{1}H-NMR (400 MHz, DMSO-d_6): δ[ppm] = 3.28–3.35 (1H, m, CH_2), 3.43–3.49 (1H, m, CH_2), 3.73 (3H, s, OCH_3), 4.74 (1H, dt, *J* = 7.7 Hz, 4.7 Hz, C*H*-OH), 5.41 (1H, d, *J* = 4.4 Hz, OH), 6.90 (2H, d, *J* = 8.6 Hz, Ar-*m*), 7.29 (2H, d, *J* = 8.6 Hz, Ar-*o*), 7.45 (2H, t, *J* = 7.3 Hz, Ar-*m*'), 7.51 (1H, t, *J* = 7.2 Hz, Ar-*p*'), 7.84 (2H, dd, *J* = 7.0 Hz, 1.6 Hz, Ar-*o*'), 8.46 (1H, t, *J* = 5.7 Hz, NH). ^{13}C-NMR (100 MHz, DMSO-d_6): δ [ppm] = 47.7, 55.0, 70.7, 113.4, 127.1, 127.2, 128.2, 131.0, 134.6, 135.8, 158.3, 166.4. GC–MS (EI, 70 eV): *m/z* = 271 (M^+, <1), 150 (39), 137 (34), 135 (76), 134 (100), 109 (20), 105 (57), 94 (19), 77 (57), 66 (7), 51 (15). The NMR data are in accordance with literature values.[42]

Environmental impact assessment

E-factor calculations were performed using the EATOS (v. 1.1) software tool,[43] while solvent demand was calculated using *Microsoft* Excel (determining the solvent use of each step separately and carrying forward the solvent demand of all intermediates). All reactions were treated as proceeding to complete conversion, hence all losses in yield are accounted for as 'unknown by-products'. In cases where the exact quantities of reagents or auxiliary materials were not given in the literature, the following estimations were used: *solvents for diluting solutions:* 3 times the initial volume, *Celite for filtration:* 0.1 g/mL of filtrate, *solvents for extraction:* 50 mL/g of crude product, *aqueous solutions for washing extracts:* 20% of extract volume, except *brine:* 10% of extract volume, *anhydrous salts for drying extracts:* 0.02 g/mL of extract volume, *solvents for recrystallisation:* 10 mL/g of crude product, *silica gel for chromatography:* 20 g/g of crude product, *eluents for chromatography:* 500 mL/g of crude product (total eluent volume). The EATOS and Excel files used for the calculations are available as Supplementary Material.

Acknowledgements

This study has been financed by the Austrian Science Fund (FWF project J3244-N17). The authors would like to thank Florian Mayer for assistance with NMR measurements, Maarten Gorseling and Remco van Oosten for general technical assistance, and Caroline Paul for proof-reading the manuscript.

Notes and references

[a] *Department of Biotechnology, Delft University of Technology, Julianalaan 136, 2628 BL Delft, The Netherlands. Fax: (+31) 152 781415; Tel: (+31) 152 781957; E-mail: j.schrittwieser@tudelft.nl, f.hollmann@tudelft.nl*
[b] *School of Advanced Studies in Science, University "G. d'Annunzio" of Chieti-Pescara, Via dei Vestini 31, 66013 Chieti, Italy*
[c] *Department of Chemistry, Organic & Bioorganic Chemistry, University of Graz, Heinrichstrasse 28, 8010 Graz, Austria*
[d] *Department of Engineering and Geology (INGEO), University "G. d'Annunzio" of Chieti-Pescara, Viale Pindaro 42, 65127 Pescara, Italy*

† Electronic Supplementary Information (ESI) available: Complete results of ADH screening, additional optimisation studies, characterisation data of Pd-NPs, additional details on the environmental assessment of tembamide syntheses, additional experimental procedures, full characterisation data of compounds isolated from the chemo-enzymatic transformations, EATOS and Excel files used in the environmental impact assessment. See DOI: 10.1039/b000000x/

1 A. Bruggink, R. Schoevaart and T. Kieboom, *Org. Process Res. Dev.*, 2003, **7**, 622–640.
2 (a) L. M. Ambrosini and T. H. Lambert, *ChemCatChem*, 2010, **2**, 1373–1380; (b) A. M. Walji and D. W. C. MacMillan, *Synlett*, 2007, 1477–1489; (c) J.-C. Wasilke, S. J. Obrey, R. T. Baker and G. C. Bazan, *Chem. Rev.*, 2005, **105**, 1001–1020; (d) J. M. Lee, Y. Na, H. Han and S. Chang, *Chem. Soc. Rev.*, 2004, **33**, 302–312.
3 For recent reviews, see: (a) H. Pellissier, *Tetrahedron*, 2013; (b) I. Oroz-Guinea and E. García-Junceda, *Curr. Opin. Chem. Biol.*, 2013, **17**, 236–249; (c) J. Park and S. Hong, *Chem. Soc. Rev.*, 2012, **41**, 6931–6943; (d) H. Pellissier, *Adv. Synth. Catal.*, 2012, **354**, 237–294; (e) R. C. Wende and P. R. Schreiner, *Green Chem.*, 2012, **14**, 1821–1849; (f) Ł. Albrecht, H. Jiang and K. A. Jørgensen, *Angew. Chem. Int. Ed.*, 2011, **50**, 8492–8509; (g) E. Ricca, B. Brucher and J. H. Schrittwieser, *Adv. Synth. Catal.*, 2011, **353**, 2239–2262; (h) C. Grondal, M. Jeanty and D. Enders, *Nat. Chem.*, 2010, **2**, 167–178; (i) M. J. Climent, A. Corma and S. Iborra, *ChemSusChem*, 2009, **2**, 500–506.
4 (a) I. Schnapperelle, W. Hummel and H. Gröger, *Chem. Eur. J.*, 2012, **18**, 1073–1076; (b) M. Poizat, I. W. C. E. Arends and F. Hollmann, *J. Mol. Catal. B: Enzym.*, 2010, **63**, 149–156; (c) E. Burda, W. Hummel and H. Gröger, *Angew. Chem. Int. Ed.*, 2008, **47**, 9551–9554.
5 For recent reviews, see: (a) A. C. Marr and S. Liu, *Trends Biotechnol.*, 2011, **29**, 199–204; (b) P. N. R. Vennestrøm, C. H. Christensen, S. Pedersen, J.-D. Grunwaldt and J. M. Woodley, *ChemCatChem*, 2010, **2**, 249–258; (c) H. C. Hailes, P. A. Dalby and J. M. Woodley, *J. Chem. Technol. Biotechnol.*, 2007, **82**, 1063–1066.
6 For recent reviews on the combination of chemo- and biocatalysis for dynamic kinetic resolution in organic media, see: (a) P. Hoyos, V. Pace and A. R. Alcántara, *Adv. Synth. Catal.*, 2012, **354**, 2585–2611; (b) J. H. Lee, K. Han, M. J. Kim and J. Park, *Eur. J. Org. Chem.*, 2010, 999–1015; (c) B. Martín-Matute and J. E. Bäckvall, *Curr. Opin. Chem. Biol.*, 2007, **11**, 226–232; (d) H. Pellissier, *Tetrahedron*, 2008, **64**, 1563–1601. For recent examples of the concurrent combination of chemo- and biocatalysis in aqueous or bi-phasic media, see: (e) Z. J. Wang, K. N. Clary, R. G. Bergman, K. N. Raymond and F. D. Toste, *Nat. Chem.*, 2013, **5**, 100–103; (f) V. Köhler, Y. M. Wilson, M. Dürrenberger, D. Ghislieri, E. Churakova, T. Quinto, L. Knörr, D. Häussinger, F. Hollmann, N. J. Turner and T. R. Ward, *Nat. Chem.*, 2013, **5**, 93–99; (g) F. G. Mutti, A. Orthaber, J. H. Schrittwieser, J. G. de Vries, R. Pietschnig and W. Kroutil, *Chem. Commun.*, 2010, **46**, 8046–8048.
7 For selected recent examples of the sequential combination of chemo- and biocatalysis in aqueous medium, see: refs. 4a and 4c; (a) A. Cuetos, F. R. Bisogno, I. Lavandera and V. Gotor, *Chem. Commun.*, 2013, **49**, 2625–2627; (b) J. S. Willemsen, J. C. M. van Hest and F. P. J. T. Rutjes, *Chem. Commun.*, 2013, **49**, 3143–3145; (c) J. M. Foulkes, K. J. Malone, V. S. Coker, N. J. Turner and J. R. Lloyd, *ACS Catalysis*, 2011, **1**, 1589–1594; (d) H. Maid, P. Böhm, S. M. Huber, W. Bauer, W. Hummel, N. Jux and H. Gröger, *Angew. Chem. Int. Ed.*, 2011, **50**, 2397–2400; (e) M. Kraußer, T. Winkler, N. Richter, S. Dommer, A. Fingerhut, W. Hummel and H. Gröger, *ChemCatChem*, 2011, **3**, 293–296; (f) K. Tenbrink, M. Seßler, J. Schatz and H. Gröger, *Adv. Synth. Catal.*, 2011, **353**, 2363–2367; (g) G. Rulli, N. Duangdee, K. Baer, W. Hummel, A. Berkessel and H. Gröger, *Angew. Chem. Int. Ed.*, 2011, **50**, 7944–7947; (h) P. N. R. Vennestrøm, E. Taarning, C. H. Christensen, S. Pedersen, J.-D. Grunwaldt and J. M. Woodley, *ChemCatChem*, 2010, **2**, 943–945; (i) E. Burda, W. Bauer, W. Hummel and H. Gröger, *ChemCatChem*, 2010, **2**, 67–72; (j) V. Gauchot, W. Kroutil and A. R. Schmitzer, *Chem. Eur. J.*, 2010, **16**, 6748–6751; (k) W. Szymanski, C. P. Postema, C. Tarabiono, F. Berthiol, L. Campbell-Verduyn, S. De Wildeman, J. G. De Vries, B. L. Feringa and D. B. Janssen, *Adv. Synth. Catal.*, 2010, **352**, 2111–2115; (l) K. Baer, M. Kraußer, E. Burda, W. Hummel, A. Berkessel and H. Gröger, *Angew. Chem. Int. Ed.*, 2009, **48**, 9355–9358; (m) A. Prastaro, P. Ceci, E. Chiancone, A. Boffi, R. Cirilli, M. Colone, G. Fabrizi, A. Stringaro and S. Cacchi, *Green Chem.*, 2009, **11**, 1929–1932; (n) R. M. Haak, F. Berthiol, T. Jerphagnon, A. J. A. Gayet, C. Tarabiono, C. P. Postema, V. Ritleng, M. Pfeffer, D. B. Janssen, A. J. Minnaard, B. L. Feringa and J. G. de Vries, *J. Am. Chem. Soc.*, 2008, **130**, 13508–13509.
8 S. C. Bergmeier, *Tetrahedron*, 2000, **56**, 2561–2576.
9 For reviews, see: (a) J. L. Vicario, D. Badía, L. Carrillo, E. Reyes and J. Etxebarria, *Curr. Org. Chem.*, 2005, **9**, 219-235; (b) K. Everaere, A. Mortreux and J. F. Carpentier, *Adv. Synth. Catal.*, 2003, **345**, 67–77; (c) D. J. Ager, I. Prakash and D. R. Schaad, *Chem. Rev.*, 1996, **96**, 835–876.
10 For a review, see: (a) F. D. Klingler, *Acc. Chem. Res.*, 2007, **40**, 1367–1376. For recent examples, see: (b) R. Kuwano, N. Kameyama and R. Ikeda, *J. Am. Chem. Soc.*, 2011, **133**, 7312–7315; (c) J. F. McGarrity and A. Zanotti-Gerosa, *Tetrahedron: Asymmetry*, 2010, **21**, 2479–2486; (d) G. Shang, D. Liu, S. E. Allen, Q. Yang and X. Zhang, *Chem. Eur. J.*, 2007, **13**, 7780–7784; (e) A. Hu and W. Lin, *Org. Lett.*, 2005, **7**, 455–458; (f) A. Lei, S. Wu, M. He and X. Zhang, *J. Am. Chem. Soc.*, 2004, **126**, 1626–1627; (g) T. Morimoto, K. Yoshikawa, M. Murata, N. Yamamoto and K. Achiwa, *Chem.*

Pharm. Bull., 2004, **52**, 1445–1450; (h) T. Ohkuma, D. Ishii, H. Takeno and R. Noyori, *J. Am. Chem. Soc.*, 2000, **122**, 6510–6511.

11 For recent examples, see: (a) H. Vázquez-Villa, S. Reber, M. A. Ariger and E. M. Carreira, *Angew. Chem. Int. Ed.*, 2011, **50**, 8979–8981; (b) O. Soltani, M. A. Ariger, H. Vázquez-Villa and E. M. Carreira, *Org. Lett.*, 2010, **12**, 2893–2895; (c) Z. Xu, S. Zhu, Y. Liu, L. He, Z. Geng and Y. Zhang, *Synthesis*, 2010, 811–817; (d) M. Watanabe, K. Murata and T. Ikariya, *J. Org. Chem.*, 2002, **67**, 1712–1715; (e) A. M. Kawamoto and M. Wills, *J. Chem. Soc., Perkin 1*, 2001, 1916–1928.

12 (a) A. Prechter, H. Gröger and M. R. Heinrich, *Org. Biomol. Chem.*, 2012, **10**, 3384–3387; (b) F. J. Quijada, F. Rebolledo and V. Gotor, *Tetrahedron*, 2012, **68**, 7670–7674; (c) R. Lihammar, R. Millet and J. E. Bäckvall, *Adv. Synth. Catal.*, 2011, **353**, 2321–2327; (d) A. Rouf, P. Gupta, M. A. Aga, B. Kumar, R. Parshad and S. C. Taneja, *Tetrahedron Asymmetry*, 2011, **22**, 2134–2143; (e) A. Chaubey, R. Parshad, P. Gupta, S. C. Taneja, G. N. Qazi, C. R. Rajan and S. Ponrathnam, *Bioorg. Med. Chem.*, 2009, **17**, 29–34.

13 (a) J. Rehdorf, M. D. Mihovilovic and U. T. Bornscheuer, *Angew. Chem. Int. Ed.*, 2010, **49**, 4506–4508; (b) J. Rehdorf, M. D. Mihovilovic, M. W. Fraaije and U. T. Bornscheuer, *Chem. Eur. J.*, 2010, **16**, 9525–9535.

14 (a) K. Baer, N. Dückers, W. Hummel and H. Gröger, *ChemCatChem*, 2010, **2**, 939–942; (b) J. Steinreiber, M. Schürmann, F. Van Assema, M. Wolberg, K. Fesko, C. Reisinger, D. Mink and H. Griengl, *Adv. Synth. Catal.*, 2007, **349**, 1379–1386; (c) J. Steinreiber, M. Schürmann, M. Wolberg, F. Van Assema, C. Reisinger, K. Fesko, D. Mink and H. Griengl, *Angew. Chem. Int. Ed.*, 2007, **46**, 1624–1626.

15 (a) T. Sehl, H. C. Hailes, J. M. Ward, R. Wardenga, E. von Lieres, H. Offermann, R. Westphal, M. Pohl and D. Rother, *Angew. Chem. Int. Ed.*, 2013, **52**, 6772–6775; (b) S. Matosevic, G. J. Lye and F. Baganz, *J. Biotechnol.*, 2011, **155**, 320–329; (c) C. U. Ingram, M. Bommer, M. E. B. Smith, P. A. Dalby, J. M. Ward, H. C. Hailes and G. J. Lye, *Biotechnol. Bioeng.*, 2007, **96**, 559–569.

16 (a) G. Sello, F. Orsini, S. Bernasconi and P. D. Gennaro, *Tetrahedron: Asymmetry*, 2006, **17**, 372–376; (b) J. S. Yadav, P. T. Reddy, S. Nanda and A. B. Rao, *Tetrahedron: Asymmetry*, 2001, **12**, 3381–3385; (c) P. A. Procopiou, G. E. Morton, M. Todd and G. Webb, *Tetrahedron: Asymmetry*, 2001, **12**, 2005–2008.

17 (a) F. Coccia, L. Tonucci, D. Bosco, M. Bressan and N. d'Alessandro, *Green Chem.*, 2012, **14**, 1073–1078; (b) F. Coccia, L. Tonucci, N. d'Alessandro, P. d'Ambrosio and M. Bressan, *Inorg. Chim. Acta*, 2013, **399**, 12–18.

18 Notably, this high chemoselectivity is in stark contrast to the hydrogenation of **3b** over Pd/C in methanol, where reductive dehalogenation was observed and **4a**·HCl was formed as the sole product in quantitative yield.

19 For studies using isolated enzymes, see: ref. 7a; (a) F. R. Bisogno, E. Garcia-Urdiales, H. Valdes, I. Lavandera, W. Kroutil, D. Suarez and V. Gotor, *Chem. Eur. J.*, 2010, **16**, 11012–11019; (b) F. R. Bisogno, I. Lavandera, W. Kroutil and V. Gotor, *J. Org. Chem.*, 2009, **74**, 1730–1732; (c) H. Ankati, Y. Yang, D. Zhu, E. R. Biehl and L. Hua, *J. Org. Chem.*, 2008, **73**, 6433–6436; (d) K. Edegger, C. C. Gruber, T. M. Poessl, S. R. Wallner, I. Lavandera, K. Faber, F. Niehaus, J. Eck, R. Oehrlein, A. Hafner and W. Kroutil, *Chem. Commun.*, 2006, **0**, 2402–2404. For studies using whole microbial cells, see: ref 16c; (e) L. C. Fardelone, J. A. R. Rodrigues and P. J. S. Moran, *J. Mol. Catal. B: Enzym.*, 2006, **39**, 9–12; (f) H. Antunes, L. d. C. Fardelone, J. A. R. Rodrigues and P. J. S. Moran, *Tetrahedron: Asymmetry*, 2004, **15**, 2615–2620; (g) J. S. Yadav, P. T. Reddy, S. Nanda and A. B. Rao, *Tetrahedron: Asymmetry*, 2001, **12**, 63–67; (h) A. E. P. M. Sorillha, M. Marques, I. Joekes, P. José, S. Moran, J. Augusto and R. Rodrigues, *Bioorg. Med. Chem. Lett.*, 1992, **2**, 191–196. For studies using carrot root as biocatalyst, see: ref. 16b; (i) J. S. Yadav, S. Nanda, P. Thirupathi Reddy and A. Bhaskar Rao, *J. Org. Chem.*, 2002, **67**, 3900–3903.

20 (a) B. Kosjek, W. Stampfer, M. Pogorevc, W. Goessler, K. Faber and W. Kroutil, *Biotechnol. Bioeng.*, 2004, **86**, 55-62; (b) W. Stampfer, B. Kosjek, C. Moitzi, W. Kroutil and K. Faber, *Angew. Chem. Int. Ed.*, 2002, **41**, 1014–1017; (c) W. Hummel, *Trends Biotechnol.*, 1999, **17**, 487–492; (d) W. Hummel, *Adv. Biochem. Eng. Biotechnol.*, 1997, **58**, 145–184; (e) R. J. Lamed and J. G. Zeikus, *Biochem. J.*, 1981, **195**, 183–190.

21 Due to the effect of the azide group on the Cahn-Ingold-Prelog priorities, enzymes with a stereoselectivity according to Prelog's rule will produce the (*R*)-enantiomer of **3a**. However, in the suppliers' catalogs these enzymes are categorised as (*S*)-selective, in accordance with the stereopreference observed with 'standard substrates' such as acetophenone or 2-octanone.

22 V. Prelog, *Pure Appl. Chem.*, 1964, **9**, 119–130.

23 Interestingly, the ADHs from *T. brockii* and *L. brevis*, which have been reported to reduce **2a**, did not give substantial conversion in our screening, despite proving active in a photometric assay on 2-propanol oxidation (for details, see ESI).

24 The oxazolidine **5** can also be turned into the main product by adding additional acetone after extraction of the crude product from the aqueous phase, and preliminary experiments have shown that more complex oxazolidines (which may contain a second chiral centre) can also be accessed by this method.

25 M.-J. Cheng, K.-H. Lee, I.-L. Tsai and I.-S. Chen, *Bioorg. Med. Chem.*, 2005, **13**, 5915–5920.

26 (a) R. A. Sheldon, *Chem. Ind.*, 1992, 903–906; (b) R. A. Sheldon, *Green Chem.*, 2007, **9**, 1273–1283; (c) R. A. Sheldon, *Chem. Commun.*, 2008, 3352–3365.

27 D.-M. Lee, J.-C. Lee, N. Jeong and K.-I. Lee, *Tetrahedron: Asymmetry*, 2007, **18**, 2662–2667.

28 A. Baeza, C. Nájera, J. M. Sansano and J. M. Saá, *Chem. Eur. J.*, 2005, **11**, 3849–3862.

29 A. Kamal, A. A. Shaik, M. Sandbhor and M. S. Malik, *Tetrahedron: Asymmetry*, 2004, **15**, 3939–3944.

30 (a) R. F. C. Brown, A. C. Donohue, W. R. Jackson and T. D. McCarthy, *Tetrahedron*, 1994, **50**, 13739–13752; (b) R. F. C. Brown, W. R. Jackson and T. D. McCarthy, *Tetrahedron: Asymmetry*, 1993, **4**, 205–206.

31 For ecological perspectives of solvent use, see: (a) K. Alfonsi, J. Colberg, P. J. Dunn, T. Fevig, S. Jennings, T. A. Johnson, H. P. Kleine, C. Knight, M. A. Nagy, D. A. Perry and M. Stefaniak, *Green Chem.*, 2008, **10**, 31–36; (b) R. A. Sheldon, *Chem. Soc. Rev.*, 2012, **41**, 1437–1451.

32 For recent articles, see: (a) K. P. Bhabak and C. Arenz, *Bioorg. Med. Chem.*, 2012, **20**, 6162–6170; (b) A. S. Aboraia, S. W. Yee, M. S. Gomaa, N. Shah, A. C. Robotham, B. Makowski, D. Prosser, A. Brancale, G. Jones and C. Simons, *Bioorg. Med. Chem.*, 2010, **18**, 4939–4946; (c) M. D. Wittman, B. Balasubramanian, K. Stoffan, U. Velaparthi, P. Liu, S. Krishnanathan, J. Carboni, A. Li, A. Greer, R. Attar, M. Gottardis, C. Chang, B. Jacobson, Y. Sun, S. Hansel, M. Zoeckler and D. M. Vyas, *Bioorg. Med. Chem. Lett.*, 2007, **17**, 974–977; (d) V. Nesterenko, K. S. Putt and P. J. Hergenrother, *J. Am. Chem. Soc.*, 2003, **125**, 14672–14673. For recent patents, see: (e) *Internat. Pat.*, WO 2012/156367, 2012; (f) *Internat. Pat.*, WO 2008/024634, 2008; (g) *Internat. Pat.*, WO 2007/078523, 2007; (h) *Internat. Pat.*, WO 2006/014357, 2006; (i) *Internat. Pat.*, WO 2005/044191, 2005; (j) *Internat. Pat.*, WO 2004/106345, 2004.

33 Since the ADH preparation is a crude cell-free extract, the exact concentration of the productive enzyme is not known. An approximation assuming 20% target protein content and a molecular weight of 30 kDa yields a concentration of 3.33 µM, corresponding to a TON of 30,000 at full conversion (100 mM substrate).

34 A. Kamal, G. B. R. Khanna, T. Krishnaji and R. Ramu, *Bioorg. Med. Chem. Lett.*, 2005, **15**, 613–615.

35 A. V. Malkov, A. J. P. S. Liddon, P. Ramírez-López, L. Bendová, D. Haigh and P. Kočovský, *Angew. Chem. Int. Ed.*, 2006, **45**, 1432–1435.

36 M. J. Bosiak and M. M. Pakulski, *Synthesis*, 2011, 316–324.

37 L. Kniežo, P. Kristian and S. Velebný, *Collect. Czech. Chem. Commun.*, 1978, **43**, 1917–1923.

38 B. T. Cho, S. K. Kang and S. H. Shin, *Tetrahedron: Asymmetry*, 2002, **13**, 1209–1217.

39 W. Becker, H. Freund and E. Pfeil, *Angew. Chem.*, 1965, **77**, 1139–1139.

40 C. Paolucci and G. Rosini, *Tetrahedron: Asymmetry*, 2007, **18**, 2923–2946.

41 A. S. Demir, C. Tanyeli, H. Aksoy, V. Gulbeyaz and A. S. Mahasneh, *Synthesis*, 1995, 1071–1073.
42 R. Somanathan, H. R. Aguilar, R. Ventura and K. M. Smith, *Synth. Commun.*, 1983, **13**, 273–280.
43 (a) M. Eissen and J. O. Metzger, *Chem. Eur. J.*, 2002, **8**, 3580–3585; (b) EATOS: Environmental Assessment Tool for Organic Syntheses, http://www.metzger.chemie.uni-oldenburg.de/eatos/english.htm, Accessed 13.06.2013.

View Article Online
DOI: 10.1039/C3GC41666F

View Article Online
DOI: 10.1039/C3GC41666F

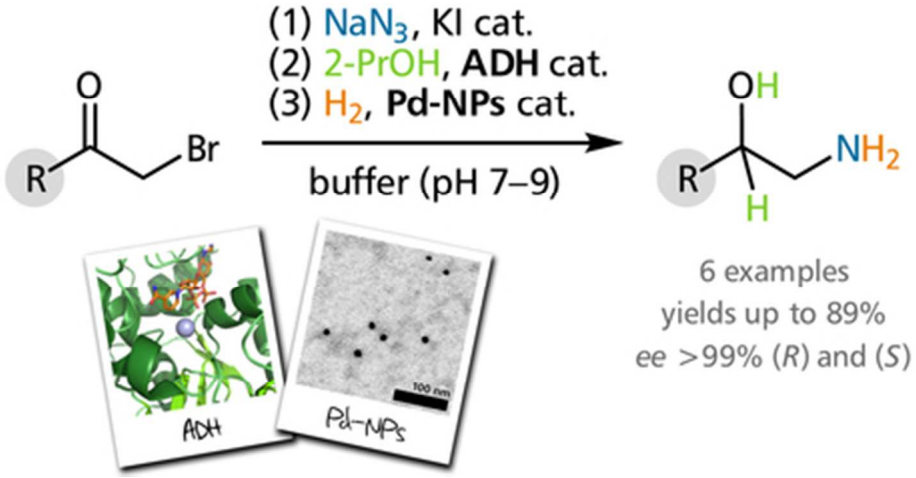

The one-pot combination of alcohol dehydrogenase (ADH) and palladium nanoparticle (Pd-NP) catalysis provides access to aromatic 1,2-amino alcohols in high yields and excellent optical purities, and allows the one-pot synthesis of the antiviral natural product (S)-tembamide with a low ecological footprint (E = 11).
39x19mm (300 x 300 DPI)